Atmos. Meas. Tech. Discuss.,
doi:10.5194/amt-2018-443-RC2, 2019
Author Response (AR) to Referee #1

We thank Referee #1 for the time spent on reviewing the manuscript and providing constructive comments. We will work on the revised manuscript accordingly. Answers to the comments are given below.

General Referee Summary: This paper reports the characterization of a new commercial laser-based HCHO sensor from Aeris Tech Inc. The 3σ detection limit of the sensor was 690 pptv with 15 min integration time. A comparison with LIF instruments was performed. The Aeris sensor provides a small and easier-to-operate HCHO sensor, which can be potentially adopted in networks. This work is interesting and meets the scope of AMT.

The new sensor takes advances in the design and data processing method, which should be included in the manuscript. Without these key informations, I do not see the compelling advances to publish in AMT in its present form.

Author Response: We appreciate the general and specific comments of Referee #1 and have added more information about the instrument design that is not proprietary or patented information. A newly-made schematic diagram now appears in the supplemental information to make the operating principle of the Aeris sensor easier to understand. We have also added a few more clarifying details about HAPP fit since the fast-fitting routine of ART fit is proprietary and closed-source (this was one of the primary reasons why HAPP fit was created for the Aeris sensor and is publicly available on GitHub).

Manuscript Changes: Modified part of Section 3: “Spectral parameters (such as the line position or the Doppler and Lorentz widths for each transition) are dynamically fixed or floated depending on a specified threshold, and spectral lines of the same molecular species are grouped together to better constrain the final fit. All spectral line information can be easily sourced from the HITRAN database. While HAPP fit itself is written in C++, the program is supported by a suite of MATLAB scripts to assist in setting up the necessary configuration files from the Aeris raw data and to process the output of HAPP fit into finalized HCHO mixing ratios.”

Comment 1: A schematic diagram is useful to make the principle of the sensor clearer.

Author Response: We agree with the referee and have added a schematic of the sensor.

Manuscript Changes: The following figure was added to supplemental information:

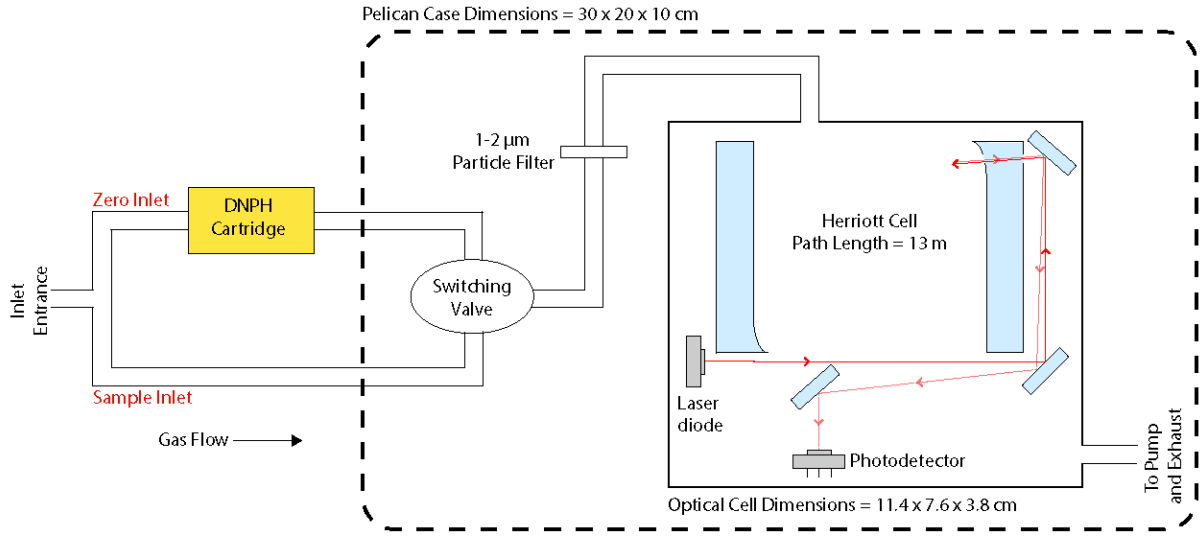

Figure S1. Schematic diagram of the absorption-based Aeris HCHO sensor. Air flows through the inlet entrance, and the switching valve either allows air to pass directly into the instrument via the sample inlet or is first scrubbed of HCHO via the zero inlet. Before entering the Herriott cell, all dust is removed from the air flow with a 1-2 µm particle filter. The patented folded Herriott cell (US Patent #10,222,595) has a path length of 13 m and dimensions of 11.4 x 7.6 x 3.8 cm (Paul, 2019). The laser diode, photodetector, filters, and mirror coatings are proprietary information.

Comment 2: Details about the multi-pass cell (the type of the cell, diameter, coating of the mirrors, and some related references) are not clear.

Author Response: Additional details about the multi-pass cell have been added to make it clearer for the reader. The multi-pass cell is a folded Herriott cell with a 13 m path length, dimensions of 11.4 x 7.6 x 3.8 cm, and a volume of 60 cm^3. The cell is also patented (US Patent #10,222,595) and details about the coating on the mirrors are proprietary. Moreover, the Herriott cell shown in Figure S1 aims to accurately capture the light path of the laser beam as it enters and exits the cell (this information was reproduced from Figures 3 and 4 of US Patent #10,222,595).

Manuscript Changes: "A proprietary folded Herriott detection cell (Paul, 2019) inside the instrument has a 1300 cm path length, a volume of 60 cm^3, and dimensions of 11.4 x 7.6 x 3.8 cm (4.5 x 3 x 1.5 inches) (Fig. 1 with a simple schematic in Fig. S1)."

Comment 3: Details about the fast-fitting routine (ART) and some related references are not clear.

Author Response: All details about the fast-fitting routine (ART) are proprietary to Aeris Technologies, which is one of the primary reasons why we developed HAPP fit as it would give the user complete control over fitting the raw 1 Hz spectral data rather than relying solely on the closed source ART fit. Developing our own non-linear least-squares fitting routine also allowed us to compare our fit to that of ART fit as we show in Eq. 2. The two fits agree to within a few percent of each other with very small offset. The fitting code for HAPP fit was further

made open source by making it available to the public via GitHub (https://github.com/nthallen/le-icosfit)

Manuscript Changes: No changes made due to the proprietary nature of ART fit.

Comment 4: Table 1, for absorption spectroscopy, what were the path lengths previously used? Then the readers can clearly see the sensitivity of the Aeris sensor with 13 m absorption pathlength and that with hundreds meters.

Author Response: We agree that including this information as a caption to Table 1 will help the reader in comparing the sensitivity of the Aeris sensor with a 13 m absorption path length to the research-grade instrumentation having path lengths that are 1 – 2 orders of magnitude higher than the Aeris.

Manuscript Changes: "The path length of the astigmatic Herriott cell in the TDLAS and QCLS instruments are 100 and 200 m, respectively. The DOAS instrument has a light path of 960 m, and the BBCEAS instrument has an effective path length of 1430 m."

Comment 5: Fig. 3, for the Allan-Werle deviation, time series measurement results need to be shown. I found some disagreement between the Allan deviation and Fig. 4 and 5. The peak-to-peak variations were obviously larger than the value getting from Allan's plot.

Author Response: We will include time series measurement results for the Allan-Werle deviation curve.

Concerning the apparent disagreement when visually comparing the results of Fig. 3 to those of Fig. 4 and 5, we note that the peak-to-peak variation at each step is not equivalent to the 1σ standard deviation at each step (which is what the Allan plot shows). When we do calculate the 1σ standard deviation at each step in Fig. 4 and 5 (note that the integration time shown on the plots is 30 s), it's 1.0 – 1.3 ppbv HCHO for the HAPP HDO fits and 1.6 – 1.7 ppbv HCHO for the HAPP CH_4 fit. These results are in general agreement with what is shown in Fig. 3 and any discrepancies could be due to the fact that Fig. 3 was derived using zero air.

Manuscript Changes: The raw data used to derive the Allan-Werle deviation curves were added as Figure S2 to the supplemental information:

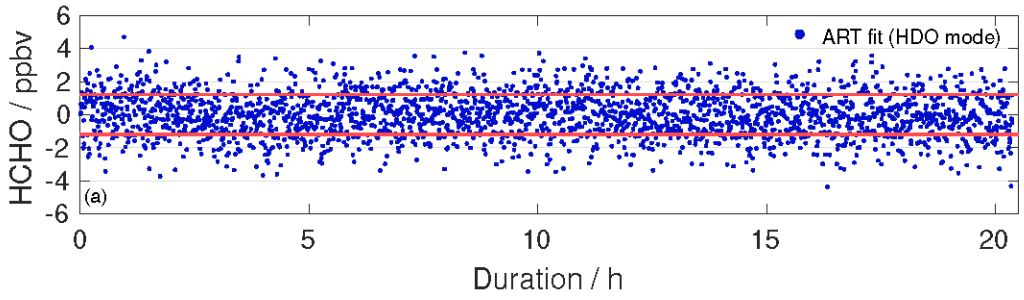

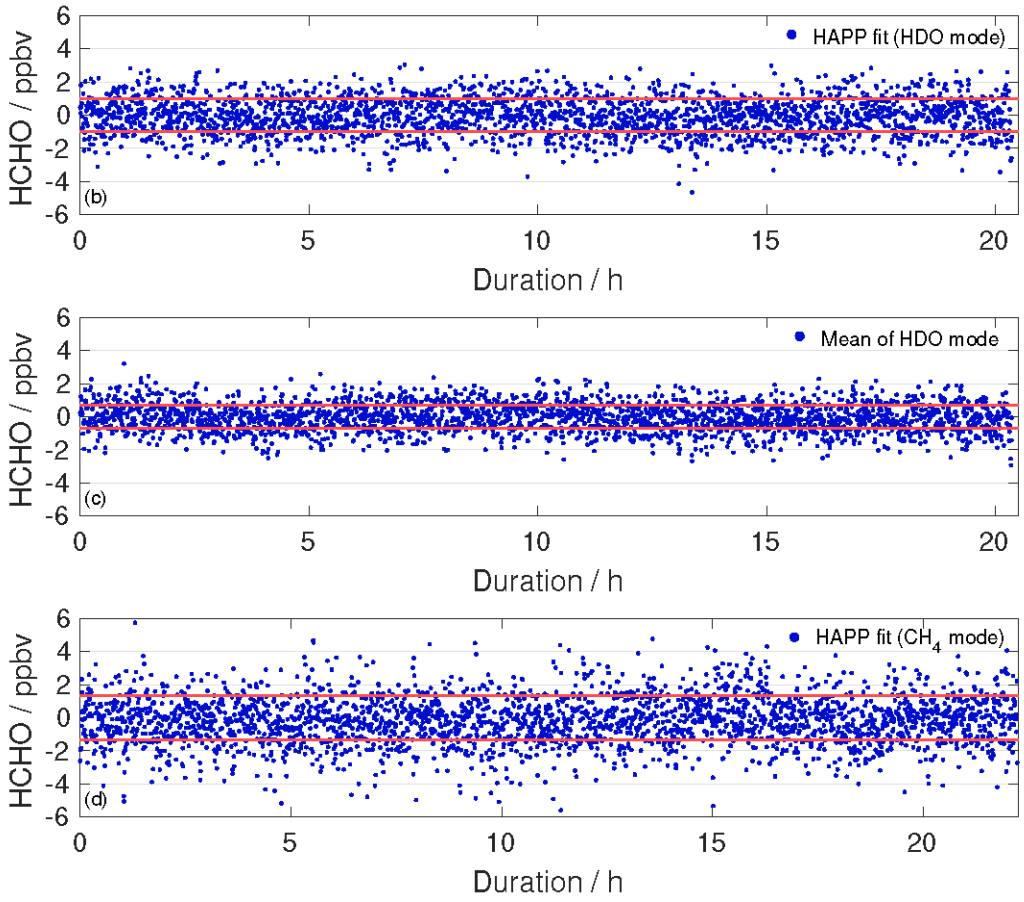

Figure S2. Raw time series data used to derive the Allan-Werle deviation curves in Figure 3. All points shown have an integration time of 30 s and were obtained by flowing ultra zero air through the Aeris sensor for a minimum of 20 h. Red lines indicate ±1σ standard deviation from the mean of the data. Raw data for (a) ART fit (HDO mode), (b) HAPP fit (HDO mode), (c) mean of HDO fits, and (d) HAPP fit (CH_4 mode).

Comment 6: Please explain the abbreviations in the manuscript, “CAFE”, “ISAF”, “FILIF”,. . .

Author Response: We agree with the referee and are defining the abbreviations for all the LIF instrumentation used in this study:
(1) CAFE stands for the **C**ompact **A**irborne **F**ormaldehyde **E**xperiment
(2) ISAF stands for the **I**n **S**itu **A**irborne **F**ormaldehyde instrument
(3) FILIF stands for the **Fi**ber **L**aser-**I**nduced **F**luorescence HCHO instrument

Manuscript Changes:

- “During a HCHO multi–hour intercomparison performed at NASA Goddard in November 2017, the Aeris sensor was operated in HDO mode and compared against two NASA LIF instruments: NASA ISAF (In Situ Airborne Formaldehyde; Cazorla et al., 2015) and NASA CAFE (Compact Airborne Formaldehyde Experiment; operating principle described in St. Clair et al., 2017).”

- "The Aeris sensor was also operated in CH_4 mode in the laboratory and compared against the Harvard FILIF (Fiber Laser-Induced Fluorescence) HCHO instrument described previously (DiGangi et al., 2011; Hottle et al., 2009)"

Comment 7: Some explanations of the 2% disagreement of the Aeris sensor and NASA CAFE and ISAF are necessary. How were these two LIF instruments calibrated? Positive offset (180 to 210 pptv) was within the detection limit of Aeris sensor.

Author Response: The reviewer is correct that the positive offset is within the detection limit of the Aeris sensor (the same also holds true for the negative offset when comparing to Harvard FILIF). That being said, all fits (both with NASA and Harvard LIF instrumentation) show an intercept that is non-zero at the 95% confidence interval, which implies that we cannot definitively rule out a real, though minor, offset whose source is unknown.

The two NASA LIF instruments were calibrated previously with a HCHO gas cylinder from Air Liquide whose concentration was verified using Fourier transform infrared (FTIR) spectroscopy (following the procedure described in Cazorla et al., 2015). The Aeris sensor was also calibrated previously at Harvard using a different HCHO gas cylinder (but this cylinder's HCHO mixing ratio was also previously verified with the same FTIR instrument as the cylinder used for calibrating the LIF instruments).

It should be noted that during the comparison of the Aeris sensor with NASA CAFE and ISAF, a small humidified stream of zero air (158 sccm) was added to the Aeris sensor only, and even though a correction was applied to account for this added dilution, it still adds in extra uncertainty. This could in part help to explain why there was a slight 2% disagreement with the Aeris sensor and NASA's LIF instruments as opposed to the 0.5 – 1% error when comparing the Aeris to Harvard FILIF (both instruments sampled the same airflow that had a small flow of (<1 sccm) of ultra-pure CH_4).

Manuscript Changes:

- "Prior to the intercomparison, all instruments were calibrated independently using HCHO gas cylinder standards that had been verified by Fourier transform infrared (FTIR) spectroscopy. In brief, the HCHO standard is verified by flowing it through an FTIR cell for several hours to allow the signal to equilibrate, and the resulting HCHO mixing ratio is scaled by a factor of 0.957 in order to tie the calibration to UV cross–sections by Meller and Moortgat (2000) (Cazorla et al., 2015)"

Atmos. Meas. Tech. Discuss.,
doi:10.5194/amt-2018-443-RC3, 2019
Author Response (AR) to Referee #2

We thank Referee #2 for the time spent on reviewing the manuscript and providing constructive comments. We will work on the revised manuscript accordingly. Answers to the comments are given below.

General Referee Summary: This paper reports the characterization of a new commercial formaldehyde sensor for monitor grade purpose. The detection limit of the instrument (3σ) was 690 pptv and 420 pptv for 15 and 60 minutes integration time, respectively. The sensor was compared to research grade Laser Induced Fluorescence instruments, which showed agreement within 10% in accuracy with up to ± 0.5 ppbv absolute difference. The sensor is useful for indoor monitor and outdoor network setup and such a paper would help to address the fundamental and technical concerns of this sensor. The authors should consider adding more discussion on how to perform a data processing method. Also, a discussion on the accuracy determination from a theoretical aspect instead of comparing with other state-of-art instruments would be helpful.

Nevertheless, this paper is well written and structured and meets the scope of AMT. Therefore, I recommend publication after minor revision.

Author Response: We appreciate the general and specific comments of Referee #2 and have added more information about HAPP fit since ART fit is proprietary to Aeris Technologies who was not willing to publish the analysis routines. This was one of the primary reasons for developing the open-source HAPP fit. An accuracy determination from LIF intercomparison was possible since all instruments were calibrated with HCHO standard gas cylinders whose concentration had been checked by Fourier transform infrared spectroscopy (FTIR) (see Cazorla et al., 2015). As such, we were able to report an accuracy of ±(10% + 0.3) ppbv and indicate that the primary factor driving this uncertainty is largely due to movements and instabilities of fringes caused by etalons in the optical train that impact how well the HCHO line is fit. Other minor factors include particles that happen to pass through the inline filter and minor molecular absorbers not listed in the HITRAN database.

Manuscript Changes: "The factor that affects the accuracy of the Aeris sensor the most likely stems from any instabilities and movements in fringes caused by the optical train's etalons (perhaps from temperature fluctuations) since any drift can subsequently impact how well the HCHO line is fit. Other matrix effects impacting the sensor's accuracy include particles that happen to pass through the inline filter and scatter the laser light as well as minor gas-phase absorbers not listed in the HITRAN database."

Comment 1: Line 15 Page 1. 'good agreement with LIF instruments from Harvard and NASA Goddard' Please be quantitative on the 'good agreement'.

Author Response: We agree with the opinion of the referee. Having added the accuracy of the sensor to the abstract (as requested by Referee #3), we have actually removed this phrasing from the abstract.

Manuscript Changes: Phrasing removed from the abstract.

Comment 2: Line 2 Page 3. Please define HITRAN. The authors should describe all the abbreviation when presented in the paper for the first time.

Author Response: HITRAN is an acronym for the **hi**gh-resolution **tran**smission molecular absorption database which compiles spectroscopic parameters for a wide range of gas-phase species in the atmosphere. HPLC stands for high-performance liquid chromatography.

Manuscript Changes:

- "A search of the nearby spectral region using HITRAN (an acronym for the *hi*gh-resolution *tran*smission molecular absorption database) shows this region to be free of strong spectral interferences from other molecular absorbers"
- "for analysis of the formaldehyde–DNPH derivative by high-performance liquid chromatography (HPLC) (Winberry et al., 1999)"

Comment 3: Line 5 Page 6. It is like a mismatch in the reference.

Author Response: We've used the same procedure described in Cazorla et al., 2015, for verifying the HCHO mixing ratio in calibration gas cylinders. The Cazorla paper uses the UV cross-sections of HCHO published by Meller and Moortgat (2000).

Manuscript Changes: No changes were made to the manuscript.

Comment 4: Figure 7a. The author could consider adding error bars on each data point to show the variability.

Author Response: We agree with the referee and have added error bars to the mean HCHO mixing ratio at each location (error bars representing ±1σ standard deviation from the mean). The raw 30 s data is also shown (in grey) to allow the reader to visually see the variability at this integration time. Additionally, we have added error bars to Figure 6a (also representing ±1σ standard deviation from the mean).

Manuscript Changes:

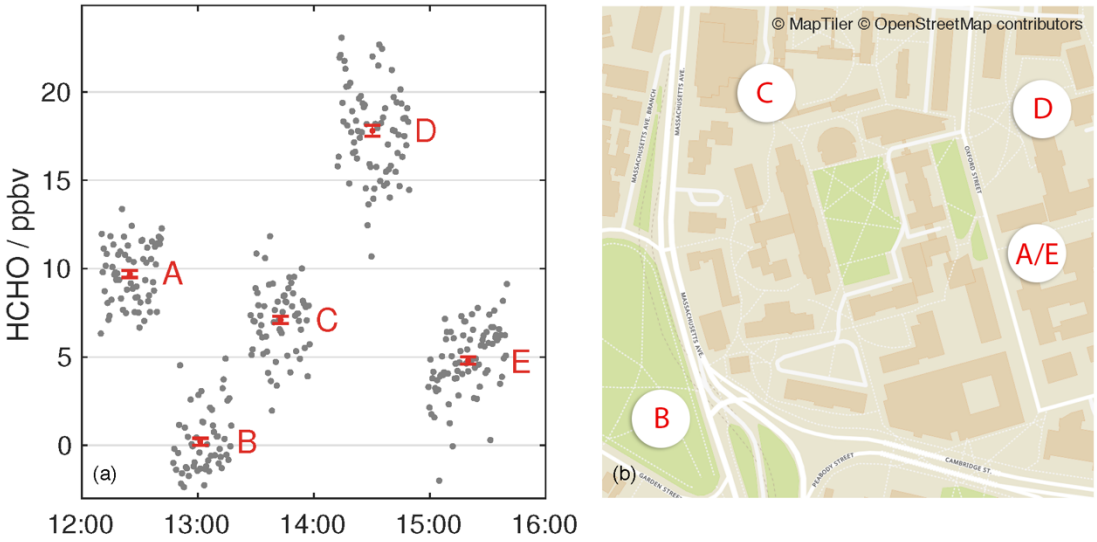

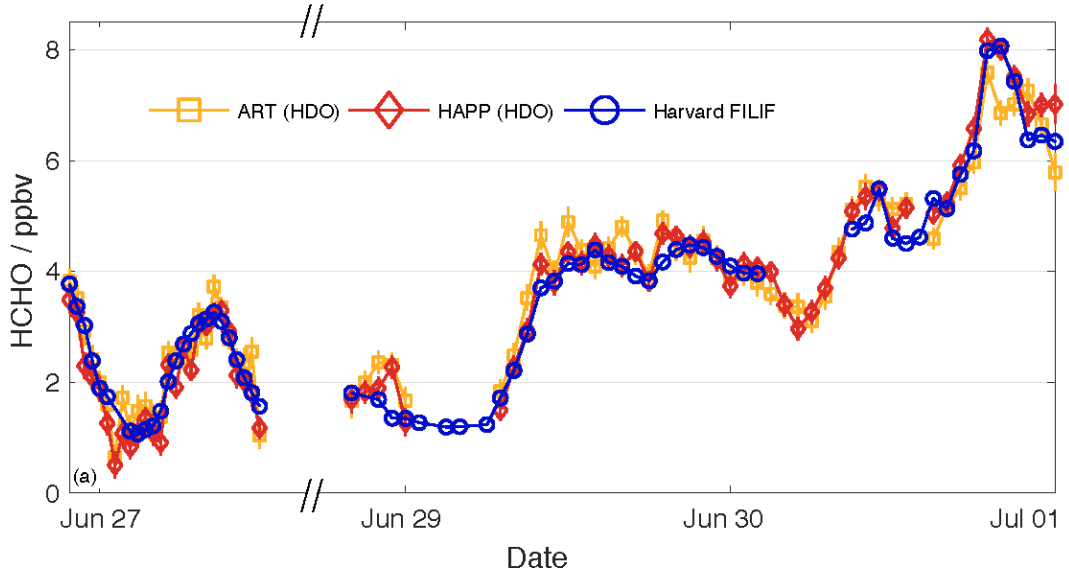

Comment 5: A schematic plot of the instrument is helpful to explain the measurement principle.

Author Response: We agree with the referee and have added a schematic of the sensor

Manuscript Changes: The following figure was added to supplemental information:

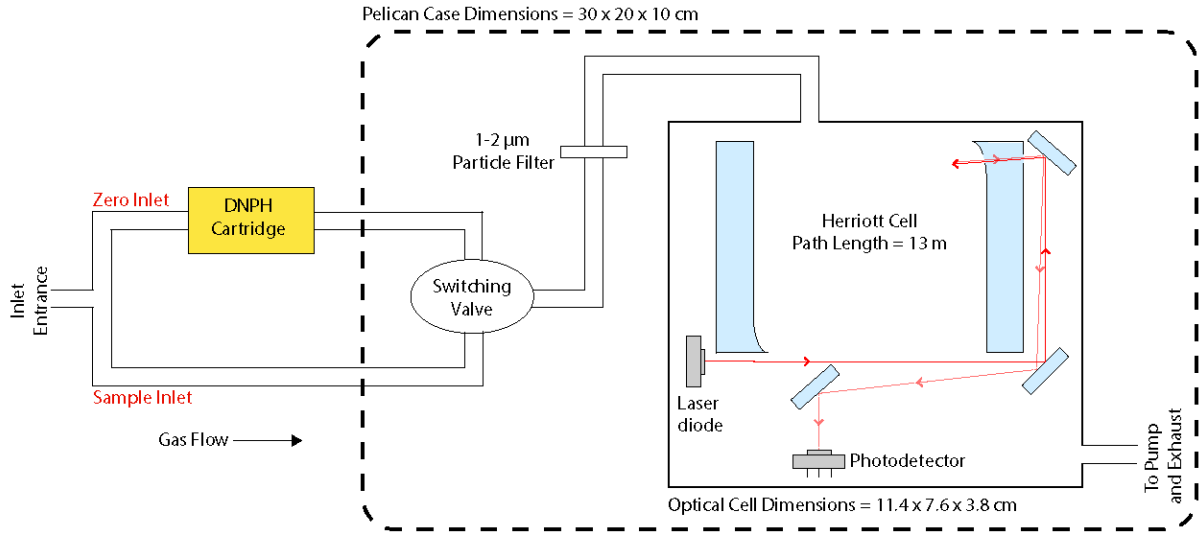

Figure S1. Schematic diagram of the absorption-based Aeris HCHO sensor. Air flows through the inlet entrance, and the switching valve either allows air to pass directly into the instrument via the sample inlet or is first scrubbed of HCHO via the zero inlet. Before entering the Herriott cell, all dust is removed from the air flow with a 1-2 µm particle filter. The patented folded Herriott cell (US Patent #10,222,595) has a path length of 13 m and dimensions of 11.4 x 7.6 x 3.8 cm (Paul, 2019). The laser diode, photodetector, filters, and mirror coatings are proprietary information.

Atmos. Meas. Tech. Discuss.,
doi:10.5194/amt-2018-443-RC1, 2019
Author Response (AR) to Referee #3

We thank Referee #3 for the time spent on reviewing the manuscript and providing constructive comments. We will work on the revised manuscript accordingly. Answers to the comments are given below.

General Referee Summary: Shutter et al. report a miniaturized instrument for monitoring grade data for formaldehyde, HCHO, based on a mid-infrared laser / Herriot cell combination. They demonstrate performance sufficient for slow time response (15-60 min) HCHO in some outdoor and (likely) many indoor environments. They compare this instrument to state of the art, research grade LIF instruments with might higher precision, showing agreement to within 10% in the slope and ±0.5 ppbv absolute difference for most conditions. They further demonstrate the utility of the instrument through a series of measurements at different locations on the Harvard campus in "personal monitoring mode".

The only significant comment is that this paper lacks a definitive statement of the instrument accuracy. Inter-comparison data are given, but there is no single statement of the accuracy of the instrument or the factors that determine it. Somewhere in the paper, perhaps after the comparison section and before the personal monitoring demonstrations, there should be paragraph that summarizes the estimates of accuracy and how it was determined. This information should also appear in the abstract.

Overall this is a short but solid paper. It will be of substantial interest to the readership of AMT. I recommend publication after attention to the comment above and the following minor comments.

Author Response: We appreciate the general and specific comments of Referee #3. We agree with the referee that an accuracy for the sensor should be quoted and also suggest the primary factor that controls the sensor's accuracy. To briefly summarize the manuscript change shown below (which has been added after the intercomparison section but before the personal monitoring demonstrations as suggested by the reviewer), we have determined an accuracy of ±(10% ± 0.3) ppbv is appropriate for the Aeris sensor (derived from ambient air sampling intercomparison) since this will be the normal operating mode of the sensor. We further believe that movements in the fringes caused etalons in the optical train (perhaps caused by temperature fluctuations) is the factor that affects the sensor's accuracy the most with other factors including particles scattering laser light and gas-phase absorbers not listed in HITRAN.

Manuscript Changes: "In determining the sensor's accuracy, there is a clear difference between how well the Aeris sensor compared to LIF instrumentation under laboratory conditions (i.e., HCHO gas standards diluted by ultra–zero air to perform stepped calibrations) (Table 2) and when sampling ambient air (Table 3). From the stepped calibrations performed in Sections 4.2.1 and 4.2.2., the mean HCHO mixing ratio at each step reported by HAPP fit was generally within ±4% of the mean value reported by LIF instrumentation. During the ambient air intercomparison with Harvard FILIF, both ART and HAPP fit showed that they were within –8% and +6%, respectively, when compared to LIF. Taking into account the 95% confidence intervals

derived from the York fits in Table 3 and a maximum offset of ~0.3 ppbv during LIF intercomparison under laboratory conditions, an accuracy of ±(10% + 0.3) ppbv should be quoted for the Aeris sensor. The factor that affects the accuracy of the Aeris sensor the most likely stems from any instabilities and movements in fringes caused by the optical train's etalons (perhaps from temperature fluctuations) since any drift can subsequently impact how well the HCHO line is fit. Other matrix effects impacting the sensor's accuracy include particles that happen to pass through the inline filter and scatter the laser light as well as minor gas-phase absorbers not listed in the HITRAN database."

Comment 1: Abstract, Line 15: "Good" agreement is not a well defined term. Abstract would be more useful if this were a number, e.g., agreement to with xx%.

Author Response: We agree with the opinion of the referee. Taking into account Comment 2, we have decided to remove this phrasing from the abstract

Manuscript Changes: "The Aeris sensor displays linear behavior ($R^2 > 0.940$) when compared with LIF instruments from Harvard and NASA Goddard."

Comment 2: Abstract, Line 17-19: Instrument precision (or LOD) is given, but accuracy is not stated. What is it?

Author Response: We completely agree with the referee. The accuracy of the sensor when sampling ambient air (as will be the case in most uses of this sensor) has been added.

Manuscript Changes: "Moreover, the accuracy of the sensor was found to be ±(10% + 0.3) ppbv when compared against LIF instrumentation sampling ambient air."

Comment 3: Page 1, Line 34: Not clear what is meant by "upwards of 15 and 40 ppbv". At least for outdoor measurement, and I suspect for indoor measurement, these appear to be high levels that would be on the upper end of a distribution, though the phrasing does not make this very clear or quantitative. Is there a better number that represents an average, especially for the indoor environment?

Author Response: The reviewer is correct that HCHO mixing ratios of 15 and 40 ppbv are at the upper end of a distribution of HCHO levels found in the outdoor and indoor environments. This distribution is seen in Figure 2 of Salthammer, T. Angew. Chemie Int. Ed., 52(12), 3320–3327, 2013. We agree the phrasing could be improved and the manuscript has been modified to give the range of HCHO levels that could be observed in indoor and outdoor locations. We are hesitant to provide an average for the outdoor environment as this shows a diurnal trend and are also hesitant about providing an average for the indoor environment since it varies widely by country and building type.

Manuscript Changes: "HCHO mixing ratios are generally higher indoors (ranging from 5 – 40 ppbv) than those measured outdoors (ranging from 0.5 – 15 ppbv with rural areas being on the lower end of the range and urban areas on the higher end) (Salthammer, 2013)."

Comment 4: Page 2, Line 6: Table 1 omits the cavity enhanced spectroscopy method of Washenfelder, AMT 9(1): p. 41-52 (2016) which reports a sensitivity and accuracy within the range of the other instruments.

Author Response: We thank the referee for mentioning this omission. Broadband cavity enhanced absorption spectroscopy (BBCEAS) has a sensitivity and accuracy that indeed is within the range of other instruments and has been added to Table 1

Manuscript Changes:

Table 1. Overview of selected in situ HCHO measurement techniques

	Method	3σ Limit of Detection (pptv)	Integration Time (s)	Accuracy (%)	Reference
Chemical	Fluorimetry[a] (Enzymatic and Hantzsch)	75–120	60–120	5–8	(Kaiser et al., 2014; Wisthaler et al., 2008)
	DNPH–HPLC	60	3600	15	(Wisthaler et al., 2008)
Spectroscopy/Spectrometry	Proton Transfer Reaction–Mass Spectrometry (PTR–MS)	300	2	10	(Wisthaler et al., 2008)
	Tunable Diode Laser Absorption Spectroscopy (TDLAS)	180	1	6	(Fried et al., 1999; Weibring et al., 2007)
	Quantum Cascade Laser Spectroscopy (QCLS)	96	1	–	(McManus et al., 2010)
	Differential Optical Absorption Spectroscopy (DOAS)	600	100	6	(Wisthaler et al., 2008)
	Broadband Cavity-Enhanced Absorption Spectroscopy (BBCEAS)	450	60	6.5	(Washenfelder et al., 2016)
	Laser–Induced Fluorescence (LIF)	30	1	10	(Cazorla et al., 2015; St. Clair et al., 2017; DiGangi et al., 2011; Hottle et al., 2009)

[a]Specified values are for Hantzsch

Comment 5: Page 2, Lines 8-9: It would be useful to the reader to translate the number to a set of actual T and RH conditions – e.g., what RH would 1500 ppmv correspond to at representative temperatures of say 25, 15 and 0°C?

Author Response: We agree with the referee and have translated the mixing ratio of water to an actual set of representative temperature and relative humidity conditions. Also, the lower limit of water vapor was raised from 1500 ppmv to 2000 ppmv after more testing of the sensor showed the need to provide a more conservative estimate in the manuscript.

Manuscript Changes: "The HCHO line is reliably found when the mixing ratio of H_2O is above 2000 ppmv (corresponding to relative humidities of 6, 12, and 33% at temperatures of 25, 15, and 0°C, respectively)."

Comment 6: Page 2, Line 33: What is the sample material for the Aeris cell? Does that material show any effects toward adsorption / desorption or reaction with H_2CO?

Author Response: While the material and the coating for the Aeris Herriott cell is proprietary, any outgassing would be accounted for since this additional background would also be part of the zero reference (measured every other 15 s under default settings) and therefore subtracted out. In our experience, we have not observed any signs that the cell is reacting with HCHO.

Manuscript Changes: "Since a zero is effectively calculated every other 15 s with default settings, the inlet and valve setup employed by the sensor helps to minimize the effects of thermal drift and other background effects (such as outgassing) on the reported HCHO mixing ratio."

Comment 7: Page 3, Lines 10-11: Is the inlet system in figure 3 external to the package in Fig 1? This seems likely, and should be noted.

Author Response: The sample and zero inlets are indeed external to the package in Fig 1 and this is now duly noted in the manuscript and in the instrument schematic (Fig S1)

Manuscript Changes: "Using default settings, the three–way valve cycles between the two external inlets every 30 s"

Figure S1 shows how the inlets are external to the portable Pelican case housing the sensor.

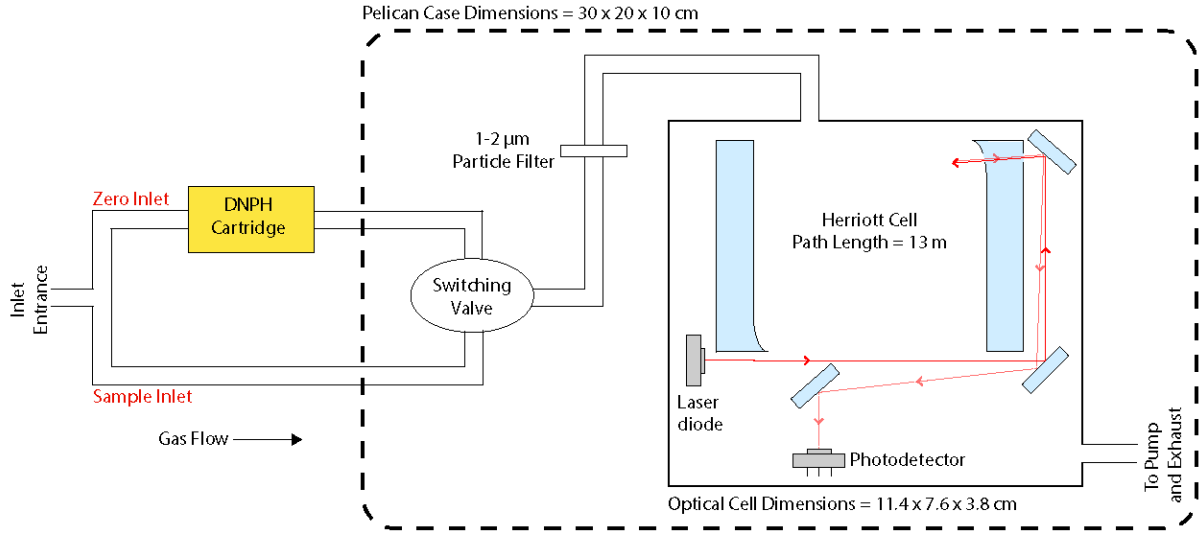

Comment 8: Page 3, Lines 12-13: The zero switch time is 15 s on / off, and the acquisition rate is 1 Hz. How much time is required to achieve stable operation after a switch? Some of the data must not be valid, limiting the actual time of measurement or duty cycle.

Author Response: The referee is correct that not all data collected during a 15 s period of sampling either the zero or sample inlet are valid. In fact, the first 7 s of data for each sampling period is ignored to prevent any hysteresis effects from the inlet previously being sampled. The manuscript has been modified to make this clearer, and the reference to the 50% duty cycle has been removed.

Manuscript Changes: "For the purpose of eliminating any hysteresis effects from the inlet previously being sampled, the first seven seconds of data are ignored for each 15 s inlet sampling period."

Comment 9: Page 3, Line 14: Is there a quantitative measure of the scrubbing efficiency of the DNPH cartridge for H_2CO? Even a limit (e.g., > xx.x%) would be useful to quote here if specified by the manufacturer or measured.

Author Response: In response to this comment, an additional experiment was performed on the Aeris sensor where a known amount of HCHO (~22 ppbv) was flowed into the sensor, but inline DNPH cartridges were on both the sample and zero inlets. From this experiment, >99.3% of the HCHO was removed by the DNPH cartridge. This scrubbing efficiency was determined with a flow rate of 750 sccm and 30% RH at 24°C.

Manuscript Changes: "containing an inline DNPH cartridge (LpDNPH S10L Cartridge, Sigma–Aldrich) that filters out all aldehydes, including more than 99% HCHO, from the air flow"

Comment 10: Page 3, Line 29: Out of curiosity, is H_2CO ever observed outgassing from new Teflon tubing, filters, or their packaging?

Author Response: Our general practice has been to use PFA tubing wherever possible since other types of tubing can outgas HCHO upon opening. That being said, sometimes the rigidity of the PFA prevents its use in some applications (like the inside of the Aeris sensor), so small lengths of flexible Tygon tubing are sometimes utilized.

Manuscript Changes: No changes were made to the manuscript.

Comment 11: Page 4, Line 24: very minor comment, but "nearly 16±9%" does not make sense, in that the number and its uncertainty is given precisely, so the word "nearly" should be omitted.

Author Response: We agree with this comment, and the manuscript has been changed.

Manuscript Changes: "HAPP fit outperforms ART fit by 16 ± 9% at all integration times"

Comment 12: Page 5, Line 20: Are the differences between fit methods a statement of the instrument accuracy? Can this be the number quoted in the abstract?

Author Response: We do not feel that the difference in fit methods presented in Equation 2 represents a statement of the instrument's accuracy since there are subsequent measurements later on that show the bounds on the accuracy should be greater than what is indicated by Equation 2.

Manuscript Changes: No changes made to manuscript.

Comment 13: Page 6, Line 13: Is there any evidence for passivation of the Aeris sensor inlet or internal surfaces, or can the entire response time be attributed to the H2CO delivery system. See question above regarding Aeris sample cell material.

Author Response: The entire time can be attributed to the HCHO delivery system since both Harvard FILIF and the Aeris sensor observe the same general equilibration time for the HCHO mixing ratio to stabilize. This can be visually observed by looking at Fig. 5a and noting how both instruments show that few ppbv rise in HCHO in the first non-zero step (starting around 10 h).

Manuscript Changes: No changes made to the manuscript.

Comment 14: Page 6, Line 21: Another very minor comment, but suggest remove "good" since the numbers given above speak quantitatively about the instrument accuracy.

Author Response: We agree with the reviewer, and the manuscript has been changed accordingly.

Manuscript Changes: "These results obtained with a different calibration tank and different LIF instrument are in excellent agreement with the ones obtained during the intercomparison at NASA Goddard, demonstrating the Aeris sensor's accuracy and linearity even at low mixing ratios."

Comment 15: Page 6, Lines 34-39: Do the authors know of any reason why the different fit methods should differ by 14%? This difference is larger than given above. Identifying the cause may help to address it. Is this number the one that should be used for instrument accuracy?

Author Response: There's a few aspects of the ambient air dataset that differ from the more controlled laboratory stepped calibrations performed with NASA and Harvard LIF instrumentation (in Sections 4.2.1 and 4.2.2). The laboratory calibrations were performed where the absolute water content was kept relatively constant and the air temperature the same, and the absolute water content and air temperature did indeed change throughout the ambient air sampling period that very likely affected the fits. Also, particles scattering laser light and gas-phase absorbers not listed in the HITRAN database could have affected measurements during the ambient air intercomparison. Moreover, as noted in Table S1 for HAPP fit, a superior fit was obtained when fitting all lines listed in the table when sampling ambient air as opposed to only the lines listed in blue when sampling HCHO diluted by ultra-zero air.

Indeed, understanding how the Aeris sensor would perform when sampling outside a controlled laboratory environment was one of the primary reasons for performing the ambient air intercomparison in Section 4.2.3. Without this test, there would be uncertainty as to how well the sensor would perform when sampling ambient air.

Manuscript Changes:

- This was added at the start of Section 4.2.3 to show how the results are different from Section 4.2.1. and Section 4.2.2: "In order to ascertain the performance of the Aeris sensor when sampling ambient air".
- Additionally, section headers were changed for Section 4.2 to better clarify for the reader the difference between the stepped calibrations (Section 4.2.1 and 4.2.2) and ambient air intercomparison (Section 4.2.3)
- The following sentence was also included at the start of Section 4.2: "Sections 4.2.1 and 4.2.2 show how the Aeris sensor compares with LIF instrumentation in the laboratory (i.e., using HCHO gas standards diluted with ultra–zero air to perform stepped calibrations); whereas, Section 4.2.3 shows how the Aeris sensor compares against LIF instrumentation from Harvard when sampling ambient outdoor air over a period of several days."

Comment 16: Page 7, Lines 24-26: While the statement is clearly correct, it is also somewhat of a throwaway. The sensor is not close to achieving the time resolution or precision for this application, but the "in its current state" implies this to be a future goal. Suggest omitting. At authors discretion.

Author Response: We agree with the reviewer since this the only time in the paper where eddy-covariance flux measurements are brought up.

Manuscript Changes: Sentence was removed from the manuscript.

A new laser–based and ultra–portable gas sensor for indoor and outdoor formaldehyde (HCHO) monitoring

Joshua D. Shutter[1], Norton T. Allen[2], Thomas F. Hanisco[4], Glenn M. Wolfe[4,5], Jason M. St. Clair[4,5], Frank N. Keutsch[1,2,3]

[1]Department of Chemistry and Chemical Biology, Harvard University, Cambridge, MA 02138, USA
[2]Harvard John A. Paulson School of Engineering and Applied Sciences, Harvard University, Cambridge, MA 02138, USA
[3]Department of Earth and Planetary Sciences, Harvard University, Cambridge, MA 02138, USA
[4]Atmospheric Chemistry and Dynamics Lab, NASA Goddard Space Flight Center, Greenbelt, MD 20771, USA
[5]Joint Center for Earth Systems Technology, University of Maryland Baltimore County, Baltimore, MD 21228, USA

Correspondence to: Joshua D. Shutter (shutter@g.harvard.edu)

Abstract. In this work, a new commercially available, laser–based, and ultra–portable formaldehyde (HCHO) gas sensor is characterized, and its usefulness for monitoring HCHO mixing ratios in both indoor and outdoor environments is assessed. Stepped calibrations and intercomparison with well–established laser–induced fluorescence (LIF) instrumentation allow a performance evaluation of the absorption-based, mid–infrared HCHO sensor from Aeris Technologies, Inc. The Aeris sensor displays linear behavior ($R^2 > 0.940$) when compared with LIF instruments from Harvard and NASA Goddard. A non–linear least–squares fitting algorithm developed independently of the sensor's manufacturer to fit the sensor's raw absorption data during post-processing further improves instrument performance. The 3σ limit of detection (LOD) for 2, 15, and 60 min integration times are 2190, 690, and 420 pptv HCHO, respectively, for mixing ratios reported in real-time, though the LOD improves to 1800, 570, and 300 pptv HCHO, respectively, during post-processing. Moreover, the accuracy of the sensor was found to be ±(10% + 0.3) ppbv when compared against LIF instrumentation sampling ambient air. This sub-ppbv precision and level of accuracy are sufficient for most HCHO levels measured in indoor and outdoor environments. While the compact Aeris sensor is currently not a replacement for the most sensitive research–grade instrumentation available, its usefulness for monitoring HCHO is clearly demonstrated.

Commented [JDS1]: Phrasing removed about "good" agreement (Referee #3 and #2)

Commented [JDS2]: Added in the 3σ LOD for a 2-min integration time

Commented [JDS3]: Statement of accuracy in abstract (Referee #3)

Commented [JDS4]: Changed to add in accuracy

1 Introduction

Understanding the production and lifetime of molecules formed from oxidation chemistry is essential to our understanding of atmospheric chemistry as a whole. Formaldehyde (HCHO) is one of the most ubiquitous tracers of volatile organic compound (VOC) oxidation chemistry since it is generally formed as VOCs are oxidized by compounds such as OH, O_3, and NO_3 (Seinfeld and Pandis, 2016). The measurement of HCHO in situ and via satellite is thus extensively used by models to constrain VOC emissions from both biogenic and anthropogenic sources worldwide and to test our understanding of VOC oxidation chemistry (Choi et al., 2010; Miller et al., 2017; Zhu et al., 2017b).

While atmospheric HCHO is primarily produced from the oxidation of VOCs (such as isoprene and CH_4), it is also produced via fuel combustion and biomass burning (Anderson et al., 1996; Holzinger et al., 1999). In the indoor environment, HCHO is released from building materials and cleaning products (Nazaroff and Weschler, 2004), and normal HCHO mixing ratios are generally higher indoors (ranging from 5 – 40 ppbv) than those measured outdoors (ranging from 0.5 – 15 ppbv with rural areas being on the lower end of the range and urban areas on the higher end) (Salthammer, 2013). Given that individuals generally spend ~90% of their time indoors (Klepeis et al., 2001) and that the United States Environmental Protection Agency (US EPA)

Commented [JDS5]: Providing a range of HCHO mixing ratios in both indoor and outdoor locations rather than just the upper end of that range. It should be noted that HCHO levels higher than those shown have also been measured, though these levels would be considered elevated (Referee #3)

classifies HCHO as a hazardous air pollutant and probable human carcinogen (Baucus, 1990; U.S. Environmental Protection Agency, 2018), the measurement of HCHO indoors is just as essential as its measurement outdoors. Recently, it has been estimated that 6,600 – 12,000 people in the US will develop cancer over their lifetime due to outdoor HCHO exposure (Zhu et al., 2017a), which implies that the number from indoor exposure should be substantially higher. The current recommended exposure limit by the National Institute for Occupational Health and Safety (NIOSH) is a time–weighted average of 16 ppbv HCHO for a 10 h workday during a 40 h workweek (Centers for Disease Control and Prevention, 2007).

Numerous chemical, spectrometric, and spectroscopic methods have been developed and utilized for the accurate and precise in situ measurement of gas–phase HCHO. Table 1 summarizes several research–grade HCHO instruments developed over the past few decades listing their accuracies as well as limits of detection (3σ) and corresponding integration times. All methods can achieve sub–ppbv detection limits within their specified integration times and accuracies better than or equal to 15%. Of all the methods, the measurement of HCHO by laser–induced fluorescence (LIF) achieves the best detection limit with the shortest integration time. Additionally, chemical derivitization is currently employed as a standard by the US EPA: The current methodology (TO–11A; 2nd ed) for determining HCHO mixing ratios instructs users to sample ambient air with pre–coated DNPH (2,4–dinitrophenylhydrazine) cartridges and then ship these cartridges to a laboratory for analysis of the formaldehyde–DNPH derivative by high-performance liquid chromatography (HPLC) (Winberry et al., 1999).

Commented [JDS6]: Acronym definition (Referee #2)

Even though these research-grade methods produce high-quality scientific data, they also require large investments of money, power, and operator time. Mass spectrometric methods have high power requirements, are large, are sensitive to humidity effects for the measurement of HCHO, and have possible cross–sensitivities (for any fragment with the same mass–to–charge ratio as ionized HCHO) (Kaiser et al., 2014; Vlasenko et al., 2010). Chemical methods suffer from reproducibility problems at ambient mixing ratios, are labor and time intensive, and require the use of acidic or hazardous reagents. Current laser-based instruments using methods such as LIF, TDLAS, QCLS, and DOAS have sufficient specifications but need knowledgeable operators and are not particularly suitable for widespread adoption in sensor networks. For applications that require a large number of instruments (such as monitoring networks), or the ability to easily and cheaply move instrumentation around from location to location (such as for studying indoor air chemistry), a smaller and easier–to–operate HCHO sensor is preferable that still compares well against research–grade instrumentation with respect to accuracy.

Toward this purpose, we characterize a new mid–IR laser–based HCHO sensor (Pico Series) from Aeris Technologies to quantify its performance against some of the best available research–grade instrumentation (i.e., LIF). Through laboratory experiments, the sensor's Allan-Werle deviation curves are calculated to determine the optimal averaging time for HCHO measurements and to assess the sensor's true 3σ limit of detection. The sensor is subsequently compared against LIF instrumentation from NASA and Harvard as a proxy for the sensor's accuracy. Finally, sensor measurements from both outdoor and indoor environments are shown to display the sensor's usefulness for monitoring HCHO.

2 Instrument description

The sensor as supplied has external dimensions of 30 x 20 x 10 cm (11.5 x 8 x 3.75 inches) and a weight of 3 kg (including batteries). A proprietary folded Herriott detection cell (Paul, 2019) inside the instrument has a 1300 cm path length, a volume of 60 cm^3, and dimensions of 11.4 x 7.6 x 3.8 cm (4.5 x 3 x 1.5 inches) (Fig. 1 with a simple schematic in Fig. S1). The pumping speed is 750 standard cubic centimeters per minute (sccm) to maintain a constant pressure of 250 mbar and a residence time of 5

Commented [JDS7]: Added more details about the multi-pass detection cell.

Also added the simple schematic of the instrument to Supplemental Information (Referee #1 and #2)

s inside the detection cell. The 6 h battery life, onboard GPS, and 15 W power consumption make the sensor highly portable and thus particularly useful for mobile and field measurements. The sensor is networkable and easy to operate, and HCHO mixing ratios can be monitored via remote desktop over the sensor's Wi–Fi network.

Using a proprietary fast-fitting routine that has been optimized to report HCHO and H_2O mixing ratios in real–time (subsequently referred to as the Aeris Real-time (ART) fit), the sensor fits a rovibrational line of HCHO at 2831.6413 cm^{-1} (with a corresponding line intensity of $5.839 \cdot 10^{-20}$ cm^{-1} / (molecule · cm^{-2})) that matches the transition chosen by Fried, et al. in their TDLAS system (Fried et al., 1999). A search of the nearby spectral region using HITRAN (an acronym for the *hi*gh-resolution *tran*smission molecular absorption database) shows this region to be free of strong spectral interferences from other molecular absorbers that would completely prevent the HCHO line from being fit under normal operating conditions (Gordon et al., 2017; Rothman et al., 2013). Additionally, ART fit uses a nearby rovibrational line of an isotopologue of water (HDO) located at 2831.8413 cm^{-1} ($3.014 \cdot 10^{-24}$ cm^{-1} / (molecule · cm^{-2})) as a spectral reference to find and fit the previously mentioned HCHO spectral feature. The HCHO line is reliably found when the mixing ratio of H_2O is above 2000 ppmv (corresponding to relative humidities of 6, 12, and 33% at temperatures of 25, 15, and 0°C, respectively). The HDO reference line, strongest HCHO spectral feature, and fringes caused by etalons in the optical train are observed in the baseline-subtracted signal depicted in Fig. 2.

Commented [JDS8]: Defining HITRAN acronym (Referee #2)

Commented [JDS9]: Changed 1500 ppmv to 2000 ppmv to provide a more conservative estimate after more testing of the sensor. Also, converted the mixing ratio of water to a representative set of temperature and relative humidities (Referee #3)

The raw signal shown in the inset of Fig. 2 is reported at a rate of 1 Hz, and the Beer-Lambert law is used to calculate rudimentary mixing ratios of HCHO and H_2O after baseline subtraction. The sensor also employs a two-inlet design and three-way valve system that allows for the measurement and subtraction of a zero during data collection. Using default settings, the three–way valve cycles between the two external inlets every 30 s. Thus, for 15 s, air flow is directed through the sample inlet, which allows air to directly flow into the detection cell after passing through a particle filter. For the other 15 s, the air flow is directed into the zero inlet containing an inline DNPH cartridge (LpDNPH S10L Cartridge, Sigma–Aldrich) that filters out all aldehydes, including more than 99% HCHO, from the air flow before it passes through the particle filter and detection cell. Since a zero is effectively calculated every other 15 s with default settings, the inlet and valve setup employed by the sensor helps to minimize the effects of thermal drift and other background effects (such as outgassing) on the reported HCHO mixing ratio. For instance, since the period of the fringes caused by the etalons in the optical train has a comparable linewidth to the spectral lines being fit, the regular zeroing helps to subtract out the fringes.

Commented [JDS10]: Mentioning that the two inlets are external to the sensor (Referee #3). Removed mention of 50% duty cycle since seven points are removed at the start of each valve switch to eliminate hysteresis from the previous inlet sampling

Commented [JDS11]: Experimentally-determined scrubbing efficiency of HCHO by a DNPH cartridge (Referee #3). Flow rate was 750 sccm and 30% RH at 24°C.

The true mixing ratio of HCHO in the sample air over a complete cycle of air flowing through the sample and zero inlets is then defined as the average of the rudimentary 1 Hz HCHO mixing ratios through the sample inlet minus the average of the rudimentary 1 Hz HCHO mixing ratios through the zero inlet for the time period immediately preceding and following the sample inlet:

$$[\mathrm{HCHO}] = \overline{1\ \mathrm{Hz\ Sample\ Inlet\ HCHO}} - \left(\frac{\overline{1\ \mathrm{Hz\ Zero\ Inlet\ HCHO}_{preceding}} + \overline{1\ \mathrm{Hz\ Zero\ Inlet\ HCHO}_{following}}}{2}\right) \quad (1)$$

For the purpose of eliminating any hysteresis effects from the inlet previously being sampled, the first seven seconds of data are ignored for each 15 s inlet sampling period. With this definition, the shortest integration time possible using default settings is 30 s. Equation (1) is subsequently used for all HCHO mixing ratios reported by the Aeris sensor.

Commented [JDS12]: Added to address the question of how much time is required to achieve stable operation after a valve switch (i.e., not all of the data collected during the 15 s sampling period is used since the first 7 s are ignored) (Referee #3)

In this paper, the particle filter was a PTFE filter membrane from Savillex (13 mm ⌀, 1–2 µm pore size). A spectral interference from newly–opened DNPH cartridges was also observed, but this disappears after 2–4 h of continuous sampling. Moreover, the cartridges last anywhere from a few days to a week of continuous use depending on sampling conditions and levels of HCHO encountered.

3 Data processing: Harvard Aeris Post-Processing (HAPP) fit

While ART fit is compatible with the sensor's limited on–board computing resources to calculate HCHO mixing ratios in real–time, the sensor also offers the option of outputting its raw 1 Hz spectral data. This raw data was used as input into a repurposed and modified non–linear least–squares fitting program originally developed for the Harvard integrated cavity output spectroscopy (ICOS) instrument (Sayres et al., 2009) in order to extend the fitting capabilities of the sensor, improve the sensor's performance in very dry conditions, and also have an open-source alternative to ART fit. Based on the Levenberg–Marquardt algorithm to fit absorption spectra, HAPP fit includes optional formulations supporting non–linear tuning rates typical of laser photodiodes, standard fits for fixed path length absorption cells, and a variety of options for fitting the baseline power curve and etalons of the Aeris sensor. Spectral parameters (such as the line position or the Doppler and Lorentz widths for each transition) are dynamically fixed or floated depending on a specified threshold, and spectral lines of the same molecular species are grouped together to better constrain the final fit. All spectral line information can be easily sourced from the HITRAN database. While HAPP fit itself is written in C++, the program is supported by a suite of MATLAB scripts to assist in setting up the necessary configuration files from the Aeris raw data and to process the output of HAPP fit into finalized HCHO mixing ratios.

Commented [JDS13]: Newly added details about HAPP fit (Referee #1 and #2)

Using HAPP fit, several additional HITRAN lines were fit in addition to the spectral lines used by ART fit. While a full list of fitted spectral lines are provided in Table S1, we notably fit the CH_4 line at 2831.9199 cm^{-1} ($1.622 \cdot 10^{-21}$ cm^{-1} / (molecule · cm^{-2})). When the absolute water content of the sampled air becomes too low, (i.e., when H_2O < 2000 ppmv – such as during a dry and cold winter) using the previously mentioned HDO line to lock onto the HCHO line becomes impractical. In this case, we found that a small flow (< 1 sccm) of ultra–pure CH_4 (Chemically Pure 99.5% Methane; Airgas) can be added to the inlet line, and the CH_4 line at 2831.9199 cm^{-1} can then be used as a spectral reference to find and fit HCHO at 2831.6413 cm^{-1}. The instrument is considered to run in "CH_4 mode" only when methane is explicitly added to the gas stream; otherwise, the instrument normally uses the water already present in air to run in "HDO mode". CH_4 mode is currently only available in HAPP fit, though a user–controlled software switch between the two modes might be added in a future update of the Aeris sensor.

4 Sensor characterization

4.1 Precision: Allan–Werle deviation and limit of detection (LOD)

The precision of the sensor was calculated for various integration times when running the Aeris sensor in both HDO and CH_4 modes. For HDO mode, a multi–hour zero (20 h) was performed using a tank of ultra–zero air (Airgas). Before the ultra–zero air entered the sensor, the air first passed through a bubbler containing distilled water so that nearly 11,000 ppm H_2O was added to the gas flow. When zeroing the sensor in CH_4 mode for a period of 22 h, a small flow (< 1 sccm) of CH_4 was added to the ultra–zero air. No water was added in CH_4 mode.

Figure 3 shows the Allan–Werle deviation curves for the Aeris sensor in both HDO and CH_4 modes. In HDO mode, HAPP fit outperforms ART fit by 16 ± 9% at all integration times achieving 1σ standard deviations of 800, 190, 100 pptv at a 1, 15, and 60 min integration times, respectively, compared to 1000, 230, and 140 pptv at 1, 15, and 60 min, respectively, for the ART fit. This

Commented [JDS14]: Removed 'nearly' (Referee #3)

is unsurprising given that the least squares algorithm in HAPP fit uses more spectral lines than ART fit which uses approximations to display the HCHO mixing ratio in real–time. Additionally, the average of the ART and HAPP HDO fits produces a generally higher precision than either fit individually (700, 660, 180, and 100 pptv at 0.5, 1, 15, and 60 min integration times, respectively). This result has borne out in repeated testing. The difference in precision between HAPP fit and the average of the HDO fits becomes smaller at longer integration times since sensor drift dominates at longer integration times as the true noise averages itself out. Thus, using the average of the two HDO fits, the detection limit of the sensor (3σ) is 540 and 300 pptv at 15 and 60 min, respectively. At essentially all integration times, the precision of HAPP fit in CH_4 mode is lower than the ART HDO fit by a factor of 1.2 ± 0.3, though it must be emphasized that CH_4 mode is the only working mode available during very dry conditions.

4.2 Accuracy: LIF intercomparison

To ascertain the linearity and accuracy of the Aeris sensor in both HDO and CH_4 modes over HCHO mixing ratios commonly measured in outdoor and indoor locations, the Aeris sensor was compared against several LIF HCHO instruments from both Harvard and NASA. Sections 4.2.1 and 4.2.2 show how the Aeris sensor compares with LIF instrumentation in the laboratory (i.e., using HCHO gas standards diluted with ultra–zero air to perform stepped calibrations); whereas, Section 4.2.3 shows how the Aeris sensor compares against LIF instrumentation from Harvard when sampling ambient outdoor air over a period of several days.

Commented [JDS15]: Suggested by Referee #3 in order to better tell the difference between the stepped calibrations with ultra-zero air and the intercomparison with Harvard FILIF when sampling ambient air.

The measurement of HCHO by LIF was first applied to in situ atmospheric measurements by Hottle et al. (2009) using a tunable, Ti:Sapphire laser. Subsequent work by DiGangi, et al. (2011) and Cazorla, et al. (2015) replaced the Ti:Sapphire laser with a narrow–bandwidth fiber laser. In brief, a fiber laser around 353 nm excites a rotational transition in the $4_0^1 A^1 A_2 \leftarrow X^1 A_1$ vibronic band of HCHO, and a photomultiplier tube (PMT) with a long–pass filter measures the resulting fluorescence at wavelengths longer than 370 nm. The mixing ratio of HCHO is proportional to the laser power–normalized PMT counts. This proportionality constant is determined from a known HCHO standard such as a permeation tube or, more recently, a HCHO gas cylinder (Cazorla et al., 2015).

4.2.1 Stepped calibration with NASA CAFE and ISAF (HDO mode)

During a HCHO multi–hour intercomparison performed at NASA Goddard in November 2017, the Aeris sensor was operated in HDO mode in the laboratory and compared against two NASA LIF instruments: NASA ISAF (In Situ Airborne Formaldehyde; Cazorla et al., 2015) and NASA CAFE (Compact Airborne Formaldehyde Experiment; operating principle described in St. Clair et al., 2017). Prior to the intercomparison, all instruments were calibrated using HCHO gas cylinder standards that had been verified by Fourier transform infrared (FTIR) spectroscopy. In brief, the HCHO standard is verified by flowing it through an FTIR cell for several hours to allow the signal to equilibrate, and the resulting HCHO mixing ratio is scaled by a factor of 0.957 in order to tie the calibration to UV cross–sections by Meller and Moortgat (2000) (Cazorla et al., 2015). During the intercomparison, a HCHO gas cylinder (~500 ppbv HCHO balance N_2; Air Liquide) was diluted by an ultra–zero air gas cylinder to levels between 0 and 25 ppbv HCHO and flowed into a common sampling manifold. To the inlet line going to the Aeris sensor, an additional flow of 158 sccm of humidified ultra–zero air was added to the total flow of 750 sccm so that the HDO line could be used as a reference. All reported values below from the Aeris sensor have already been corrected for this additional dilution factor.

Commented [JDS16]: Abbreviation definition (Referee #1)

Commented [JDS17]: Mentioning how the instruments were calibrated (Referee #1)

The ART and HAPP fits were compared for the entirety of the intercomparison. Their relationship is shown (with 95% confidence intervals computed) in Eq. (2):

$$[\text{HAPP HDO fit}] = (0.98 \pm 0.01) \cdot [\text{ART HDO fit}] - (0.15 \pm 0.14) \quad (2)$$

In general, the HAPP HDO fit computes mixing ratios that are 2% lower than those calculated by ART fit ($R^2 = 0.941$) along with a negative offset of 150 pptv. A correlation plot between the two HDO fits is shown in Fig. S3.

Figure 4 shows correlation plots of the HAPP HDO fit versus the NASA ISAF and CAFE instruments, and Fig. S4 shows the time series of this same data with an integration time of 30 s, which is the lowest possible integration time for the Aeris sensor at its default settings. With this integration time, the 1σ standard deviation (using the zero air segment) of the Aeris sensor was 1000 pptv while those of NASA ISAF and CAFE were 3 and 40 pptv, respectively. Using a bivariate linear regression fit formulated by York, et al. (2004), Table 2 shows the relationships between the Aeris sensor and NASA LIF instruments. In both comparisons, the Aeris instrument calculates mixing ratios that are ~2% higher than the mixing ratios reported by NASA ISAF or CAFE. The Aeris sensor also displays a slight positive offset of 180 to 210 pptv when compared against the NASA instrumentation.

4.2.2 Stepped calibration with Harvard FILIF (CH_4 mode)

The Aeris sensor was also operated in CH_4 mode in the laboratory and compared against the Harvard FILIF (Fiber Laser-Induced Fluorescence) HCHO instrument described previously (DiGangi et al., 2011; Hottle et al., 2009) but with several modifications which will be briefly outlined. First, the 32-pass White–type multi–pass detection cell has been replaced with a more stable and easier–to–align single–pass detection cell as described and used in Cazorla, et al. (2015). The single–pass cell is coated in an ultra–black carbon nanotube coating (Singularity Black; NanoLab, Inc.) that minimizes noise in the photomultiplier tube due to scattered photons from the 353 nm laser (NovaWave Technologies, TFL Series). Upgrades to the instrument's electronics and software (now running QNX) have also been performed to increase its reliability as it samples at a default rate of 10 Hz.

Commented [JDS18]: Abbreviation definition (Referee #1)

This intercomparison utilized a HCHO gas cylinder (600 ppbv HCHO balance N_2; Air Liquide) that was diluted with ultra–zero air (Airgas) to levels between 0 and 50 ppbv HCHO and flowed into a common sampling line. A check of the mixing ratio of HCHO in the calibration tank by FTIR showed that the scaled FTIR–derived mixing ratio (524 ± 15 ppbv HCHO) was 13% less than what was quoted on the tank, so the scaled FTIR–derived value was used for this comparison. To the 5000 sccm gas flow from the ultra–zero air tank, < 1 sccm of ultra–pure CH_4 (Chemically Pure 99.5% Methane; Airgas) was added so that the Aeris sensor was running in CH_4 mode.

Figure 5 shows the results of the multi–day stepped intercomparison between Harvard FILIF and the Aeris sensor. In the first non-zero HCHO step, both the Aeris sensor and Harvard FILIF instrument show that the HCHO mixing ratio took several hours to stabilize at 15.3 ppbv. This is likely due to the HCHO gas passivating the stainless–steel surfaces of the gas regulator and MKS mass flow controller (500 sccm full scale) even though the latter was coated in a FluoroPel omniphobic coating (FluoroPel 800; Cytonix). All other surfaces were PFA plastic. This highlights the need to perform HCHO calibrations over several hours to allow for passivation of all surfaces.

At 30 s, the Aeris sensor had a 1σ precision of 1350 pptv as opposed to 22 pptv for Harvard FILIF during this experiment. The difference does improve at a 1 h integration time when the 1σ precision for the Aeris becomes 230 pptv and that of FILIF is 8.5 pptv. Table 2 shows the results of a linear regression of the HCHO mixing ratios from the Aeris sensor versus those reported by Harvard FILIF. The regression shows the Aeris sensor reporting the HCHO mixing ratio as ~1% higher when compared to FILIF with a negative offset of 150 pptv. These results obtained with a different calibration tank and different LIF instrument are in excellent agreement with the ones obtained during the intercomparison at NASA Goddard, demonstrating the Aeris sensor's accuracy and linearity even at low mixing ratios.

Commented [JDS19]: Removed the qualitative wording of "good" (Referee #3)

4.2.3 Ambient air intercomparison with Harvard FILIF (HDO mode)

In order to ascertain the performance of the Aeris sensor when sampling ambient air, the sensor and Harvard FILIF were collocated in Cambridge, MA to sample outdoor air for several days at the end of June 2018 (both instruments used the same inlet line). The ART and HAPP fit hourly averages for HCHO in HDO mode are compared against the mixing ratios from Harvard FILIF in Fig. 6. Though conditions during the measurement period were generally partly or mostly cloudy with highs reaching 33°C by the end of the week, it was punctuated by rain showers that lasted from the evening of June 27 to the evening of June 28. During this time, both ART and HAPP fit HCHO underpredicted FILIF by ~500 pptv, though this is a sampling error due to water condensing onto the optics of the sensor (as evidenced by some slight water damage observed on the optical coating following this experiment). This problem can be alleviated in the future with an inline water trap and ensuring that the sensor is not substantially colder than the temperature of the ambient air.

Commented [JDS20]: Setting up why the results obtained in Section 4.2.3 may not necessarily be the same as those obtained in Sections 4.2.1 and 4.2.2 (Referee #3)

Considering all hours except for the rain showers (n = 63 h), 87% of the HAPP fit hourly mixing ratios are within ±0.5 ppbv of FILIF and 100% are within ±1 ppbv. Similarly, 73% and 98% of the ART fit hourly mixing ratios are within ±0.5 and ±1 ppbv of FILIF, respectively. Table 3 shows the results of a linear regression of ART and HAPP fit HCHO mixing ratios versus those reported by FILIF. The regression demonstrates that the ART fit mixing ratios were ~8% lower than FILIF with a positive offset of 440 pptv. On the other hand, the HAPP fit mixing ratios were ~6% higher than FILIF with a negative offset of 160 pptv. With both fits within ±10% of FILIF, these results readily demonstrate the utility of using the Aeris sensor as a monitor for ambient levels of HCHO in the environment.

In determining the sensor's accuracy, there is a clear difference between how well the Aeris sensor compared to LIF instrumentation under laboratory conditions (i.e., HCHO gas standards diluted by ultra–zero air to perform stepped calibrations) (Table 2) and when sampling ambient air (Table 3). From the stepped calibrations performed in Sections 4.2.1 and 4.2.2., the mean HCHO mixing ratio at each step reported by HAPP fit was generally within ±4% of the mean value reported by LIF instrumentation. During the ambient air intercomparison with Harvard FILIF, both ART and HAPP fit showed that they were within –8% and +6%, respectively, when compared to LIF. Taking into account the 95% confidence intervals derived from the York fits in Table 3 and a maximum offset of ~0.3 ppbv during LIF intercomparison under laboratory conditions, an accuracy of ±(10% + 0.3) ppbv should be quoted for the Aeris sensor. The factor that affects the accuracy of the Aeris sensor the most likely stems from any instabilities and movements in fringes caused by the optical train's etalons (perhaps from temperature fluctuations) since any drift can subsequently impact how well the HCHO line is fit. Other matrix effects impacting the sensor's accuracy include particles that happen to pass through the inline filter and scatter the laser light as well as minor gas-phase absorbers not listed in the HITRAN database.

Commented [JDS21]: This entire discussion of accuracy has been included thanks to the feedback from Referee #3 and #2.

5 Portability demonstration

One of the advantages of the Aeris sensor over other instruments is its light weight and portability, so a demonstration of the portability of the Aeris sensor was performed by carrying it around as a personal HCHO exposure monitor around the Harvard campus. Figure 7 shows a map of the locations visited. Even though the data was collected during a winter month in Massachusetts when the air is generally cold and dry (which would necessitate running in CH_4 mode), the sensor operated in HDO mode due to an unseasonal local temperature of 22°C and 63% relative humidity. The sensor's batteries did not have to be recharged during the measurement period.

The five measurement sites (HAPP HDO fit HCHO mixing ratios and ±1σ standard deviation of the mean for each location in parentheses) were (A) an office space (9.7 ± 0.2 ppbv), (B) an urban park (0.2 ± 0.2 ppbv), (C) a cafeteria during lunchtime (7.1 ± 0.2 ppbv), (D) the ant collection room in the Harvard Natural History Museum (17.8 ± 0.3 ppbv), and (E) laboratory space in the Mallinckrodt Chemistry Building (4.8 ± 0.2 ppbv). All locations were indoors except for B. This sampling demonstrates the portability of the sensor in both indoor and outdoor locations and its potential use in indoor air chemistry studies. Even though the LIF instruments have much higher precision than the Aeris sensor, this simple experiment around the Harvard campus would have been cumbersome and logistically impractical given the size and power requirements of the LIF instruments and other spectroscopic and spectrometric methods mentioned previously. Moreover, all the mixing ratios were calculated in real–time unlike offline HCHO measurement methods such as the current EPA standard methodology.

6 Conclusions

While the Aeris sensor is not a replacement for research–grade instrumentation for measuring HCHO in some applications, its ease–of–use, portability, and cost make the sensor a prime candidate for use in a variety of routine monitoring applications. The 3σ limit of detection at a 15 min integration time is 690 and 570 pptv HCHO for ART and HAPP fits, respectively, which improves to 420 and 300 pptv HCHO at a 60 min integration time. With sub-ppbv precision at these times, the sensor can easily distinguish between ambient levels of HCHO normally found in outdoor and indoor locations. Moreover, the ambient outdoor air intercomparison with Harvard FILIF in Fig. 6 shows that the Aeris sensor hourly HCHO is generally within ±0.5 ppbv of the HCHO mixing ratio reported by LIF instrumentation. This intercomparison demonstrates that the sensor is a viable alternative for ambient air monitoring networks or perhaps indoor air chemistry studies.

As discussed in the text, the sensor can operate in both HDO and CH_4 mode. While HDO mode is preferable in most cases, during cold weather operation when the air is dry, it is recommended to run the Aeris sensor in CH_4 mode by adding a < 1 sccm flow from an ultra–pure CH_4 gas tank. While this makes the sensor less portable, it ensures that data can still be collected in these conditions. The need for a spare CH_4 gas tank would be made obsolete if a small CH_4 reference cell were added to the sensor or the etalons were reduced or better characterized by software to improve the signal–to–noise ratio on the HDO spectral line.

Code and data availability

HAPP fit can be provided upon request by email to Norton T. Allen (allen@huarp.harvard.edu) or via GitHub (https://github.com/nthallen/le-icosfit). Data used in this paper can be provided upon request by email to Joshua D. Shutter (shutter@g.harvard.edu).

Author contributions

JDS led this work, designed and carried out experiments, completed the data analysis, and wrote the paper with input from all co-authors. NTA wrote HAPP fit and assisted JDS with data analysis. TFH oversees all NASA LIF instrumentation and approved intercomparison efforts at NASA Goddard. GMW provided data from NASA ISAF and designed experiments during the NASA Goddard intercomparison in November-December 2017. JMSC provided data from NASA CAFE. As principal investigator, FNK provided supervision and acquired financial support for this project.

Competing interests

The authors declare that they have no conflict of interest.

Acknowledgements

The authors acknowledge Aeris Technologies (Joshua B. Paul, Jerome Thiebaud, Stephen So, and James J. Scherer) for helpful discussions along with the development and fabrication of the sensor. Additionally, the authors acknowledge Joshua L. Cox for his assistance during the HCHO intercomparison at NASA Goddard in November–December 2017. This material is based upon work supported by the National Science Foundation Graduate Research Fellowship under Grant No. DGE–1745303.

References

Anderson, L. G., Lanning, J. A., Barrell, R., Miyagishima, J., Jones, R. H. and Wolfe, P.: Sources and sinks of formaldehyde and acetaldehyde: An analysis of Denver's ambient concentration data, Atmos. Environ., 30(12), 2113–2123, doi:10.1016/1352-2310(95)00175-1, 1996.

Baucus, M.: S. 1630 - 101st Congress: Clean Air Act Amendments of 1990, United States Congress, Washington, DC., 1990.

Cazorla, M., Wolfe, G. M., Bailey, S. A., Swanson, A. K., Arkinson, H. L. and Hanisco, T. F.: A new airborne laser-induced fluorescence instrument for in situ detection of formaldehyde throughout the troposphere and lower stratosphere, Atmos. Meas. Tech., 8(2), 541–552, doi:10.5194/amt-8-541-2015, 2015.

Centers for Disease Control and Prevention: NIOSH Pocket Guide to Chemical Hazards, [online] Available from: https://www.cdc.gov/niosh/npg/npgd0293.html (Accessed 30 September 2018), 2007.

Choi, W., Faloona, I. C., Bouvier-Brown, N. C., McKay, M., Goldstein, A. H., Mao, J., Brune, W. H., LaFranchi, B. W., Cohen, R. C., Wolfe, G. M., Thornton, J. A., Sonnenfroh, D. M. and Millet, D. B.: Observations of elevated formaldehyde over a forest canopy suggest missing sources from rapid oxidation of arboreal hydrocarbons, Atmos. Chem. Phys., 10(18), 8761–8781, doi:10.5194/acp-10-8761-2010, 2010.

St. Clair, J. M., Swanson, A. K., Bailey, S. A., Wolfe, G. M., Marrero, J. E., Iraci, L. T., Hagopian, J. G. and Hanisco, T. F.: A new non-resonant laser-induced fluorescence instrument for the airborne in situ measurement of formaldehyde, Atmos. Meas. Tech., 10(12), 4833–4844, doi:10.5194/amt-10-4833-2017, 2017.

DiGangi, J. P., Boyle, E. S., Karl, T., Harley, P., Turnipseed, A., Kim, S., Cantrell, C., Maudlin, R. L., Zheng, W., Flocke, F., Hall, S. R., Ullmann, K., Nakashima, Y., Paul, J. B., Wolfe, G. M., Desai, A. R., Kajii, Y., Guenther, A. and Keutsch, F. N.: First direct measurements of formaldehyde flux via eddy covariance: Implications for missing in-canopy formaldehyde sources, Atmos. Chem. Phys., 11(20), 10565–10578, doi:10.5194/acp-11-10565-2011, 2011.

Fried, A., Wert, B. P., Henry, B. and Drummond, J. R.: Airborne tunable diode laser measurements of formaldehyde,

Spectrochim. Acta Part A Mol. Biomol. Spectrosc., 55(10), 2097–2110, doi:10.1016/S1386-1425(99)00082-7, 1999.

Gordon, I. E., Rothman, L. S., Hill, C., Kochanov, R. V., Tan, Y., Bernath, P. F., Birk, M., Boudon, V., Campargue, A., Chance, K. V., Drouin, B. J., Flaud, J.-M., Gamache, R. R., Hodges, J. T., Jacquemart, D., Perevalov, V. I., Perrin, A., Shine, K. P., Smith, M.-A. H., Tennyson, J., Toon, G. C., Tran, H., Tyuterev, V. G., Barbe, A., Császár, A. G., Devi, V. M., Furtenbacher, T., Harrison, J. J., Hartmann, J.-M., Jolly, A., Johnson, T. J., Karman, T., Kleiner, I., Kyuberis, A. A., Loos, J., Lyulin, O. M., Massie, S. T., Mikhailenko, S. N., Moazzen-Ahmadi, N., Müller, H. S. P., Naumenko, O. V., Nikitin, A. V., Polyansky, O. L., Rey, M., Rotger, M., Sharpe, S. W., Sung, K., Starikova, E., Tashkun, S. A., VanderAuwera, J., Wagner, G., Wilzewski, J., Wcisło, P., Yu, S. and Zak, E. J.: The HITRAN2016 molecular spectroscopic database, J. Quant. Spectrosc. Radiat. Transf., 203, 3–69, doi:10.1016/J.JQSRT.2017.06.038, 2017.

Holzinger, R., Warneke, C., Hansel, A., Jordan, A., Lindinger, W., Scharffe, D. H., Schade, G. and Crutzen, P. J.: Biomass burning as a source of formaldehyde, acetaldehyde, methanol, acetone, acetonitrile, and hydrogen cyanide, Geophys. Res. Lett., 26(8), 1161–1164, doi:10.1029/1999GL900156, 1999.

Hottle, J. R., Huisman, A. J., DiGangi, J. P., Kammrath, A., Galloway, M. M., Coens, K. L. and Keutsch, F. N.: A laser induced fluorescence-based instrument for in-situ measurements of atmospheric formaldehyde, Environ. Sci. Technol., 43(3), 790–795, doi:10.1021/es801621f, 2009.

Kaiser, J., Li, X., Tillmann, R., Acir, I., Holland, F., Rohrer, F., Wegener, R. and Keutsch, F. N.: Intercomparison of Hantzsch and fiber-laser-induced-fluorescence formaldehyde measurements, Atmos. Meas. Tech., 7(6), 1571–1580, doi:10.5194/amt-7-1571-2014, 2014.

Klepeis, N. E., Nelson, W. C., Ott, W. R., Robinson, J. P., Tsang, A. M., Switzer, P., Behar, J. V, Hern, S. C. and Engelmann, W. H.: The National Human Activity Pattern Survey (NHAPS): A resource for assessing exposure to environmental pollutants, J. Expo. Sci. Environ. Epidemiol., 11(3), 231–252, doi:10.1038/sj.jea.7500165, 2001.

MapTiler and OpenStreetMap Contributors: Maputnik v1.5.0, [online] Available from: https://www.openstreetmap.org, https://openmaptiles.org, and https://maputnik.github.io, 2018. OpenStreetMap data is available under the Open Database License and cartography is licensed as CC BY-SA.

McManus, J. B., Zahniser, M. S., Nelson, D. D., Shorter, J. H., Herndon, S. C., Wood, E. C. and Wehr, R.: Application of quantum cascade lasers to high-precision atmospheric trace gas measurements, Opt. Eng., 49(11), 111124, doi:10.1117/1.3498782, 2010.

Meller, R. and Moortgat, G. K.: Temperature dependence of the absorption cross sections of formaldehyde between 223 and 323 K in the wavelength range 225-375 nm, J. Geophys. Res. Atmos., 105(D6), 7089–7101, doi:10.1029/1999JD901074, 2000.

Miller, C. C., Jacob, D. J., Marais, E. A., Yu, K., Travis, K. R., Kim, P. S., Fisher, J. A., Zhu, L., Wolfe, G. M., Hanisco, T. F., Keutsch, F. N., Kaiser, J., Min, K. E., Brown, S. S., Washenfelder, R. A., González Abad, G. and Chance, K.: Glyoxal yield from isoprene oxidation and relation to formaldehyde: Chemical mechanism, constraints from SENEX aircraft observations, and interpretation of OMI satellite data, Atmos. Chem. Phys., 17(14), 8725–8738, doi:10.5194/acp-17-8725-2017, 2017.

Nazaroff, W. W. and Weschler, C. J.: Cleaning products and air fresheners: Exposure to primary and secondary air pollutants, Atmos. Environ., 38(18), 2841–2865, doi:10.1016/J.ATMOSENV.2004.02.040, 2004.

Paul, J. B.: Compact Folded Optical Multipass System, US Patent #10,222,595. 2019.

Rothman, L. S., Gordon, I. E., Babikov, Y., Barbe, A., Benner, D. C., Bernath, P. F., Birk, M., Bizzocchi, L., Boudon, V., Brown, L. R., Campargue, A., Chance, K., Cohen, E. A., Coudert, L. H., Devi, V. M., Drouin, B. J., Fayt, A., Flaud, J.-M., Gamache, R. R., Harrison, J. J., Hartmann, J.-M., Hill, C., Hodges, J. T., Jacquemart, D., Jolly, A., Lamouroux, J., Le Roy, R. J., Li, G., Long, D. A., Lyulin, O. M., Mackie, C. J., Massie, S. T., Mikhailenko, S., Müller, H. S. P., Naumenko, O. V., Nikitin, A.

V., Orphal, J., Perevalov, V., Perrin, A., Polovtseva, E. R., Richard, C., Smith, M. A. H., Starikova, E., Sung, K., Tashkun, S., Tennyson, J., Toon, G. C., Tyuterev, V. G. and Wagner, G.: The HITRAN2012 molecular spectroscopic database, J. Quant. Spectrosc. Radiat. Transf., 130, 4–50, doi:10.1016/j.jqsrt.2013.07.002, 2013.

Salthammer, T.: Formaldehyde in the ambient atmosphere: From an indoor pollutant to an outdoor pollutant?, Angew. Chemie Int. Ed., 52(12), 3320–3327, doi:10.1002/anie.201205984, 2013.

Sayres, D. S., Moyer, E. J., Hanisco, T. F., St Clair, J. M., Keutsch, F. N., O'Brien, A., Allen, N. T., Lapson, L., Demusz, J. N., Rivero, M., Martin, T., Greenberg, M., Tuozzolo, C., Engel, G. S., Kroll, J. H., Paul, J. B. and Anderson, J. G.: A new cavity based absorption instrument for detection of water isotopologues in the upper troposphere and lower stratosphere, Rev. Sci. Instrum., 80(4), 044102, doi:10.1063/1.3117349, 2009.

Seinfeld, J. H. and Pandis, S. N.: Atmospheric Chemistry and Physics: From Air Pollution to Climate Change, 3rd ed., Wiley., 2016.

U.S. Environmental Protection Agency: Risk Assessment for Carcinogenic Effects, 2018.

Vlasenko, A., Macdonald, A. M., Sjostedt, S. J. and Abbatt, J. P. D.: Formaldehyde measurements by Proton transfer reaction - Mass spectrometry (PTR-MS): Correction for humidity effects, Atmos. Meas. Tech., 3(4), 1055–1062, doi:10.5194/amt-3-1055-2010, 2010.

Washenfelder, R. A., Attwood, A. R., Flores, J. M., Zarzana, K. J., Rudich, Y. and Brown, S. S.: Broadband cavity-enhanced absorption spectroscopy in the ultraviolet spectral region for measurements of nitrogen dioxide and formaldehyde, Atmos. Meas. Tech., 9(1), 41–52, doi:10.5194/amt-9-41-2016, 2016.

Weibring, P., Richter, D., Walega, J. G. and Fried, A.: First demonstration of a high performance difference frequency spectrometer on airborne platforms, Opt. Express, 15(21), 13476–13495, doi:10.1364/OE.15.013476, 2007.

Winberry, W. T., Tejada, S., Lonneman, B. and Kleindienst, T.: Compendium of Methods for the Determination of Toxic Organic Compounds in Ambient Air: Compendium Method TO-11A, 2nd ed., U.S. Environmental Protection Agency, Cincinnati, OH., 1999.

Wisthaler, A., Apel, E. C., Bossmeyer, J., Hansel, A., Junkermann, W., Koppmann, R., Meier, R., Müller, K., Solomon, S. J., Steinbrecher, R., Tillmann, R. and Brauers, T.: Technical Note: Intercomparison of formaldehyde measurements at the atmosphere simulation chamber SAPHIR, Atmos. Chem. Phys., 8(8), 2189–2200, doi:10.5194/acp-8-2189-2008, 2008.

York, D., Evensen, N. M., Martínez, M. L. and De Basabe Delgado, J.: Unified equations for the slope, intercept, and standard errors of the best straight line, Am. J. Phys., 72(3), 367–375, doi:10.1119/1.1632486, 2004.

Zhu, L., Jacob, D. J., Keutsch, F. N., Mickley, L. J., Scheffe, R., Strum, M., González Abad, G., Chance, K., Yang, K., Rappenglück, B., Millet, D. B., Baasandorj, M., Jaeglé, L. and Shah, V.: Formaldehyde (HCHO) as a hazardous air pollutant: Mapping surface air concentrations from satellite and inferring cancer risks in the United States, Environ. Sci. Technol., 51(10), 5650–5657, doi:10.1021/acs.est.7b01356, 2017a.

Zhu, L., Mickley, L. J., Jacob, D. J., Marais, E. A., Sheng, J., Hu, L., Abad, G. G. and Chance, K.: Long-term (2005–2014) trends in formaldehyde (HCHO) columns across North America as seen by the OMI satellite instrument: Evidence of changing emissions of volatile organic compounds, Geophys. Res. Lett., 44(13), 7079–7086, doi:10.1002/2017GL073859, 2017b.

Table 1. Overview of selected in situ HCHO measurement techniques

	Method	3σ Limit of Detection (pptv)	Integration Time (s)	Accuracy (%)	Reference
Chemical	Fluorimetry[a] (Enzymatic and Hantzsch)	75–120	60–120	5–8	(Kaiser et al., 2014; Wisthaler et al., 2008)
	DNPH–HPLC	60	3600	15	(Wisthaler et al., 2008)
Spectroscopy/Spectrometry	Proton Transfer Reaction–Mass Spectrometry (PTR–MS)	300	2	10	(Wisthaler et al., 2008)
	Tunable Diode Laser Absorption Spectroscopy (TDLAS)[b]	180	1	6	(Fried et al., 1999; Weibring et al., 2007)
	Quantum Cascade Laser Spectroscopy (QCLS)[b]	96	1	–	(McManus et al., 2010)
	Differential Optical Absorption Spectroscopy (DOAS)[b]	600	100	6	(Wisthaler et al., 2008)
	Broadband Cavity-Enhanced Absorption Spectroscopy (BBCEAS)[b]	450	60	6.5	(Washenfelder et al., 2016)
	Laser–Induced Fluorescence (LIF)	30	1	10	(Cazorla et al., 2015; St. Clair et al., 2017; DiGangi et al., 2011; Hottle et al., 2009)

[a]Specified values are for Hantzsch. [b]The path length of the astigmatic Herriott cell in the TDLAS and QCLS instruments are 100 and 200 m, respectively. The DOAS instrument has a light path of 960 m, and the BBCEAS instrument has an effective path length of 1430 m.

Commented [JDS22]: BBCEAS instrument added (Referee #3)

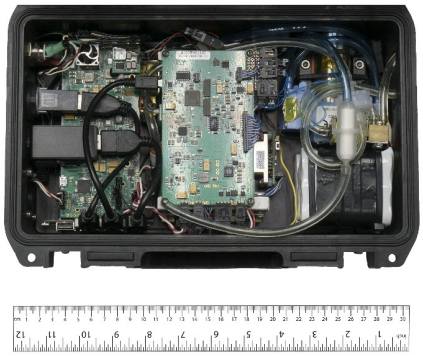

Figure 1. Internal view of the mid–IR, absorption-based HCHO sensor from Aeris Technologies. The sensor fits inside a Pelican case that provides for easy transport and mobility.

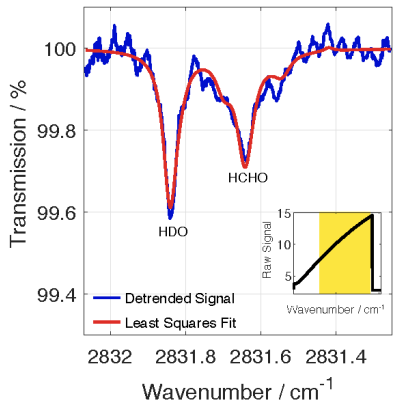

Figure 2. When the H_2O mixing ratio is above 2000 ppmv, the HDO line at 2831.8413 cm^{-1} rises above the fringing caused by etalons in the detection cell so that the position of the HCHO line at 2831.6413 cm^{-1} can be reliably located and the spectral line fit. The fit depicted corresponds to a HCHO mixing ratio around 800 ppbv. (*inset*) 1 Hz raw data from the sensor before baseline subtraction. The yellow shaded region corresponds to the wavelength range being fit.

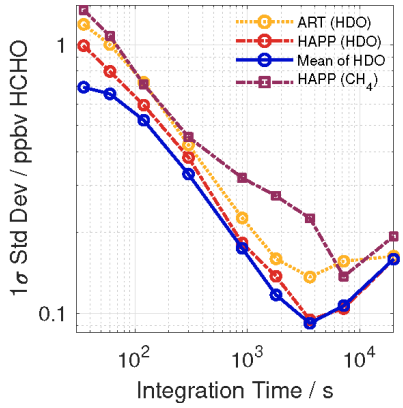

Figure 3. Allan–Werle deviation curves HCHO measurements by the Aeris sensor with different fitting modes. In HDO mode, ART and HAPP fits are shown as well as their mean. In CH_4 mode, the HAPP fit is shown. The average of the ART and HAPP fits in HDO mode produces the lowest 1σ standard deviation with a minimum of 100 pptv for a 1 h integration time. Table S2 lists 1σ standard deviations at selected integration times and Fig. S2 shows the raw time series data used to derive the Allan-Werle deviation curves.

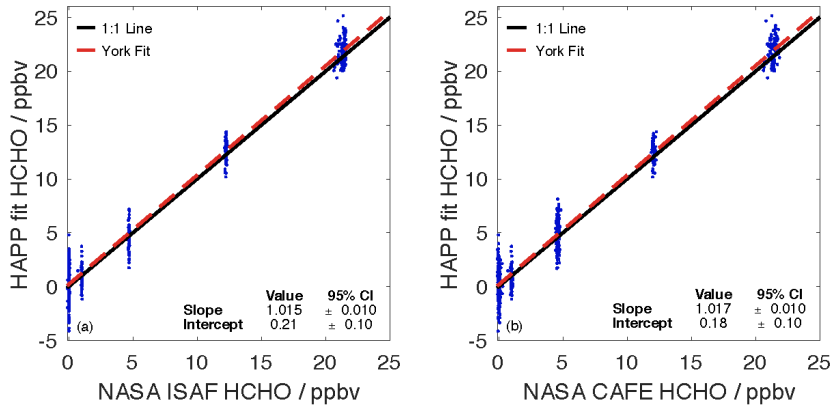

Figure 4. Correlation plots between the HAPP HDO fit and two NASA LIF instruments: (a) NASA ISAF (R^2 = 0.979) and (b) NASA CAFE (R^2 = 0.976). A time series plot for the stepped intercomparison performed at NASA Goddard is located in the supplemental information (Fig. S4).

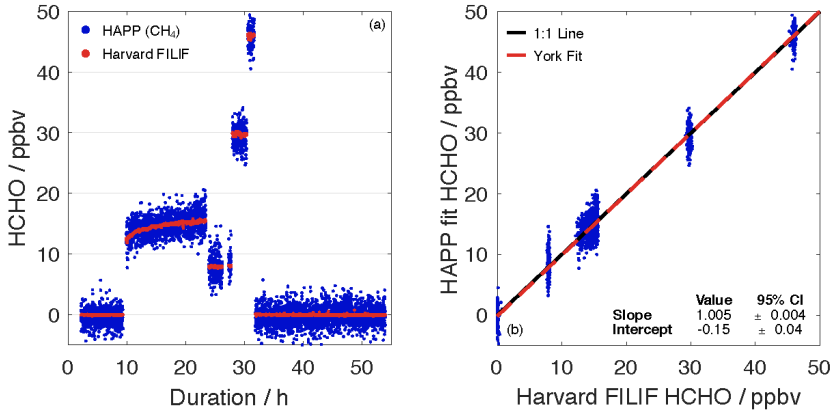

Figure 5. (a) Time series of the Aeris sensor (HAPP CH_4 fit) and Harvard FILIF during a multi–day stepped intercomparison. All data are reported with an integration time of 30 s. (b) Correlation plot between the Aeris sensor (HAPP CH_4 fit) and Harvard FILIF (R^2 = 0.980).

Table 2. Regression analyses for Aeris sensor vs LIF instruments under laboratory conditions calculated with a 95% confidence interval

		Linear Fit (*[Aeris] = m·[LIF instrument] + b*)		
	Sensor Mode	m	b	R^2
NASA ISAF	HDO	1.015 ± 0.010	0.21 ± 0.10	0.979
NASA CAFE	HDO	1.017 ± 0.010	0.18 ± 0.10	0.976
Harvard FILIF	CH_4	1.005 ± 0.004	-0.15 ± 0.04	0.980

Bivariate least squares regressions were calculated according to the method of York, et al (2004). HAPP fits were used for reporting the HCHO mixing ratio from the Aeris sensor. Laboratory conditions denote diluting HCHO gas standards using ultra–zero air. Units are in ppbv.

Commented [JDS23]: Added error bars (Referee #2)

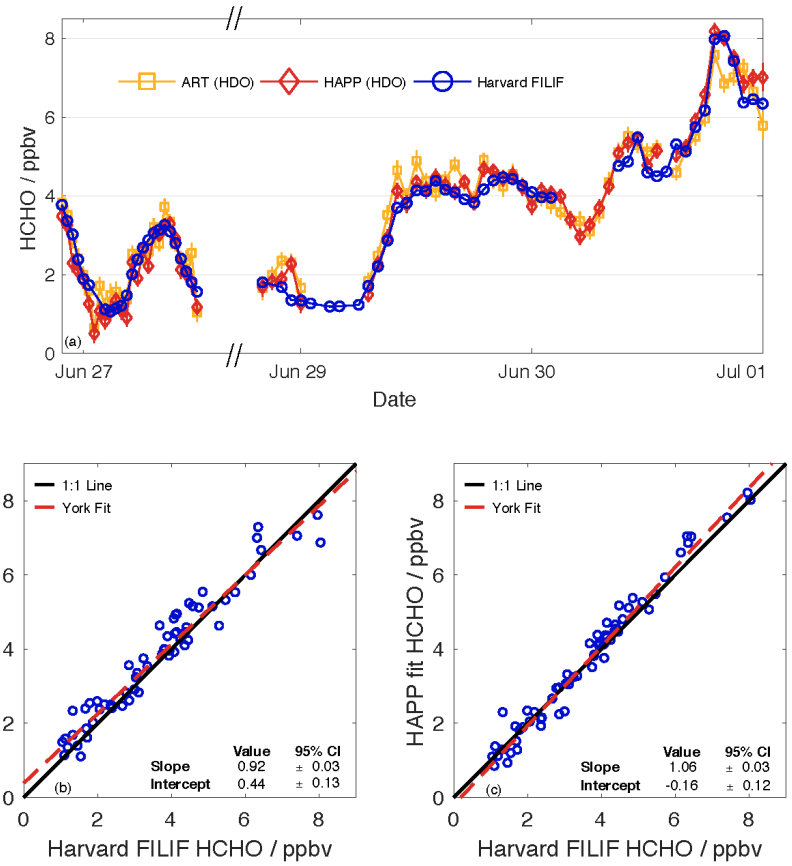

Figure 6. (a) Collocated, multi–day sampling of ambient air in Cambridge, MA, by Harvard FILIF and the Aeris sensor (HDO mode). Ticks represent midnight (00:00) on the specified date. All data is reported with an integration time of 60 min. From the evenings of June 27–28, the area experienced rain showers that caused both the ART and HAPP fits to underestimate the HCHO mixing ratio by ~0.5 ppbv due to water condensing on the optics. Data from the Aeris sensor was also removed (1) during the early hours of June 29 due to replacement of the DNPH cartridge and (2) during the afternoon of June 30 due to zeroing of the sensor with ultra–zero air. Correlation plots comparing Harvard FILIF with (b) ART fit (R^2 = 0.940) and (c) HAPP fit (R^2 = 0.974).

Table 3. Regression analysis for Aeris sensor vs Harvard FILIF sampling ambient air calculated with a 95% confidence interval

	Linear Fit (*[Aeris] = m·[Harvard FILIF] + b*)		
	m	b	R^2
ART fit	0.92 ± 0.03	0.44 ± 0.13	0.940
HAPP fit	1.06 ± 0.03	-0.16 ± 0.12	0.974

Bivariate least squares regressions were calculated according to the method of York, et al (2004). Units are in ppbv.

Commented [JDS24]: Changed to show error bars (representing ±1σ standard deviation of the mean) for each location (Referee #2)

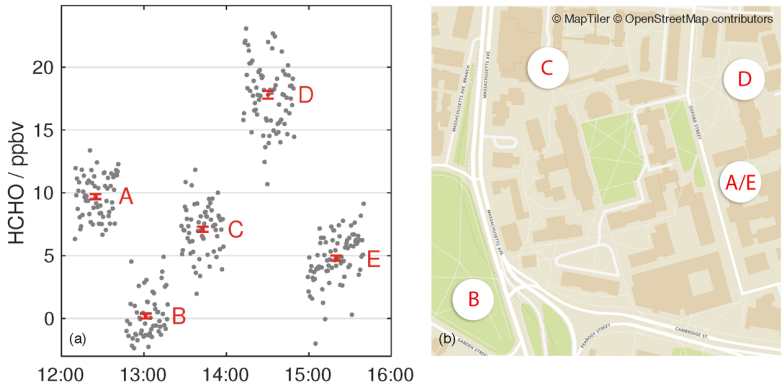

Figure 7. (a) Aeris sensor (operating in HAPP fit HDO mode) used as a HCHO personal exposure monitor for several hours on a single battery charge around the Harvard campus in Cambridge, MA. All times EDT. Locations included (A) office space (N = 64 points), (B) urban park (N = 55 points), (C) cafeteria (N = 62 points), (D) museum space (N = 75 points), and (E) lab space (N = 82 points). The data from HAPP fit is displayed with the raw 30 s data (grey) as well as the average and ±1σ standard deviation of the mean for each location (red). Data is not shown when the sensor was transported from one location to another. (b) Map data © OpenStreetMap contributors. Schema from OpenMapTiles.org (MapTiler and OpenStreetMap Contributors, 2018).

Supplement of

A new laser–based and ultra–portable gas sensor for indoor and outdoor formaldehyde (HCHO) monitoring

J. D. Shutter et al.

Correspondence to: J. D. Shutter (shutter@g.harvard.edu)

Table S1. Frequencies and line intensities of HITRAN lines used by HAPP fits

Wavenumber / cm^{-1}	Molecular species	Spectral line intensity (296 K) / cm^{-1} / molecule · cm^{-2}
2831.2598	CH_4	2.863e-22
2831.2701	CH_4	2.308e-25
2831.2737	HCHO	2.101e-20
2831.2780	CH_4	2.471e-22
2831.2802	CH_4	3.408e-25
2831.3160	CH_4	3.394e-23
2831.3259	HCHO	2.900e-21
2831.3366	CH_4	2.603e-25
2831.3501	CH_4	3.240e-25
2831.3550	HCHO	1.420e-20
2831.3657	CH_4	3.587e-25
2831.4055	HDO	1.812e-28
2831.4097	HDO	1.812e-28
2831.4209	**CH_4**	**1.553e-23**
2831.5393	**HCHO**	**5.622e-21**
2831.5534	CH_4	8.870e-25
2831.5576	**HCHO**	**5.543e-21**
2831.5616	**CH_4**	**1.549e-23**
2831.5801	HDO	4.140e-28
2831.6413	**HCHO**	**5.839e-20**
2831.6879	HCHO	1.499e-21
2831.6892	HCHO	1.499e-21
2831.6961	CH_4	6.671e-25
2831.6989	**HCHO**	**1.410e-20**
2831.8134	**HCHO**	**6.509e-21**
2831.8214	CH_4	3.671e-24
2831.8413	**HDO**	**3.014e-24**
2831.8516	CH_4	1.983e-24
2831.8906	HDO	9.812e-28
2831.8948	H_2O	1.595e-28
2831.9199	**CH_4**	**1.622e-21**
2831.9569	HDO	2.713e-27

Spectral lines from the same molecular species are fitted together rather than independently. Lines bolded in blue were used in experiments that utilized ultra-zero air, and it was discovered that all the lines listed produced a more superior fit than only the lines bolded in blue when sampling ambient air. Spectral frequencies and line intensities were accessed using HITRAN on the Web (http://hitran.iao.ru/) (Rothman et al., 2013).

Table S2. 1σ standard deviation for Aeris sensor at various integration times. All values are in pptv and were obtained by either (1) bubbling ultra-zero air (1000 sccm) though water (HDO mode) or (2) adding chemically-pure 99.5% CH_4 (< 1 sccm) to 5000 sccm ultra-zero air (CH_4 mode).

Integration time / s	ART fit HDO mode / pptv HCHO	HAPP fit HDO mode / pptv HCHO	Average of the two HDO modes / pptv HCHO	HAPP fit CH_4 mode / pptv HCHO
30	1200	1000	700	1350
60	1000	800	660	1100
120	730	600	530	720
300	430	380	330	460
900	230	190	180	320
1800	160	140	120	280
3600	140	100	100	230
7200	160	110	110	140
20000	170	160	160	200

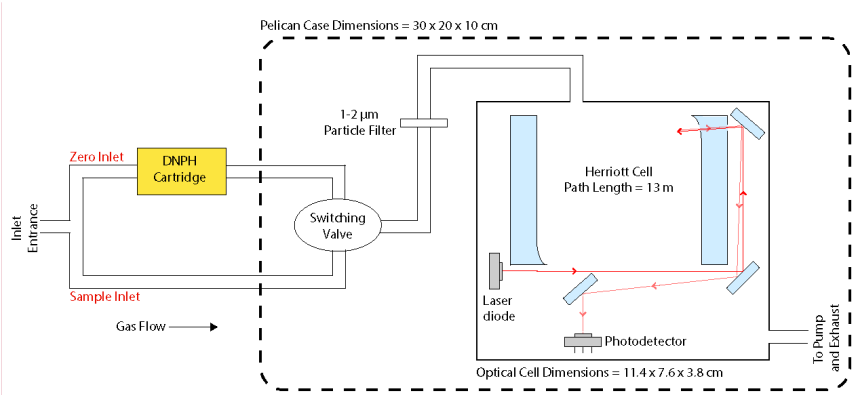

Figure S1. Schematic diagram of the Aeris sensor. Air flows through the inlet entrance, and the switching valve either allows air to pass directly into the instrument via the sample inlet or is first scrubbed of HCHO via the zero inlet. Before entering the Herriott cell, all dust is removed from the air flow with a 1-2 µm particle filter. The patented folded Herriott cell (US Patent #10,222,595) has a path length of 13 m and dimensions of 11.4 x 7.6 x 3.8 cm (Paul, 2019). The laser diode, photodetector, filters, and mirror coatings are proprietary information.

Commented [JDS1]: This schematic has been added to help aid the reader in understanding the operating principle of the instrument (Referee #1, 2, and 3)

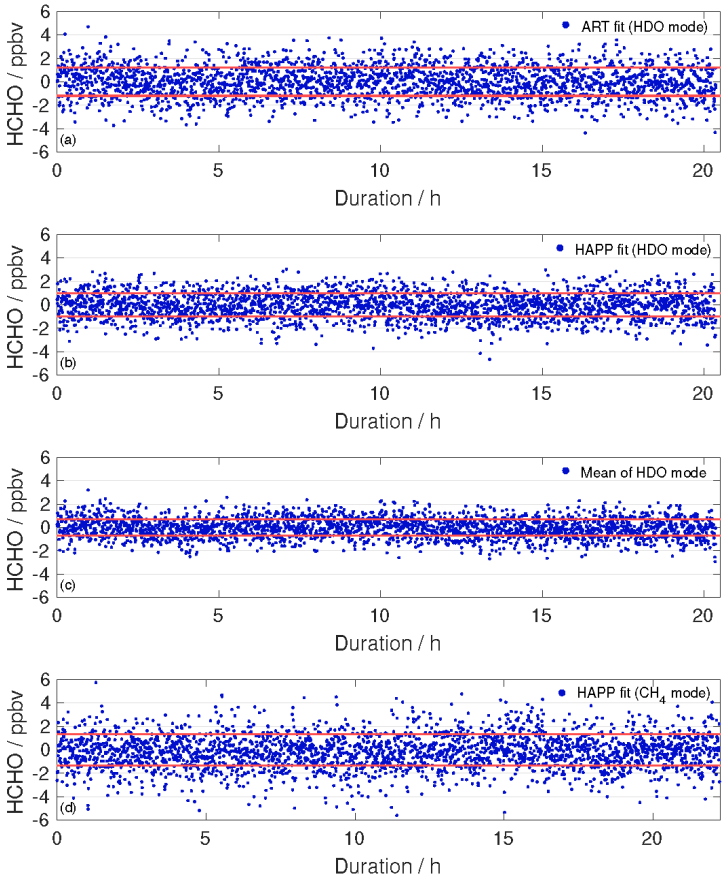

Figure S2. Raw time series data used to derive the Allan-Werle deviation curves in Figure 3. All points shown have an integration time of 30 s and were obtained by flowing ultra zero air through the Aeris sensor for a minimum of 20 h. Red lines indicate ±1σ standard deviation from the mean of the data. Raw data for (a) ART fit (HDO mode), (b) HAPP fit (HDO mode), (c) mean of HDO fits, and (d) HAPP fit (CH_4 mode).

Commented [JDS2]: Added at the suggestion of Referee #1.

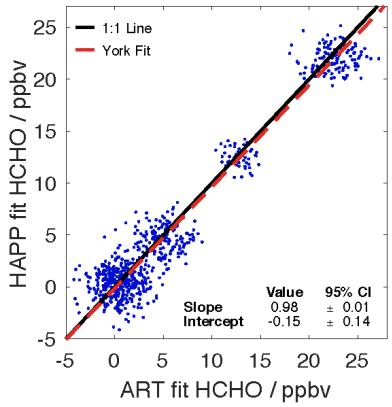

Figure S3. Correlation plot between the Aeris Real-time (ART) fit and the Harvard Aeris-Post Processing (HAPP) fit ($R^2 = 0.941$).

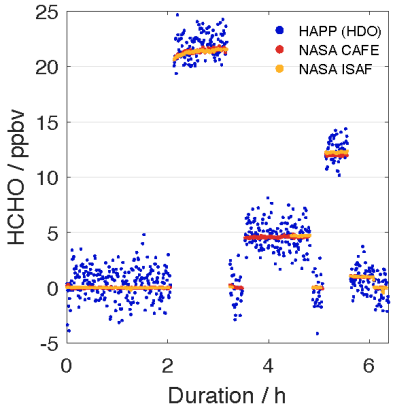

Figure S4. Time series showing the HCHO mixing ratios from the Aeris sensor (HAPP HDO fit) and NASA ISAF and CAFE during a multi–hour stepped intercomparison performed at NASA Goddard in November 2017. All data are reported with an integration time of 30 s.

Paul, J. B.: Compact Folded Optical Multipass System, US Patent #10,222,595. 2019.

Rothman, L. S., Gordon, I. E., Babikov, Y., Barbe, A., Benner, D. C., Bernath, P. F., Birk, M., Bizzocchi, L., Boudon, V., Brown, L. R., Campargue, A., Chance, K., Cohen, E. A., Coudert, L. H., Devi, V. M., Drouin, B. J., Fayt, A., Flaud, J.-M., Gamache, R. R., Harrison, J. J., Hartmann, J.-M., Hill, C., Hodges, J. T., Jacquemart, D., Jolly, A., Lamouroux, J., Le Roy, R. J., Li, G., Long, D. A., Lyulin, O. M., Mackie, C. J., Massie, S. T., Mikhailenko, S., Müller, H. S. P., Naumenko, O. V., Nikitin, A. V., Orphal, J., Perevalov, V., Perrin, A., Polovtseva, E. R., Richard, C., Smith, M. A. H., Starikova, E., Sung, K., Tashkun, S., Tennyson, J., Toon, G. C., Tyuterev, V. G. and Wagner, G.: The HITRAN2012 molecular spectroscopic database, J. Quant. Spectrosc. Radiat. Transf., 130, 4–50, doi:10.1016/J.JQSRT.2013.07.002, 2013.